Colloquium: The quest for high-conductance DNA

R. G. Endres

Center for Computational Sciences and Computer Science & Mathematics Division, Oak Ridge National Laboratory, Oak Ridge, Tennessee 37831-6114, USA

D. L. Cox and R. R. P. Singh

Department of Physics and Center for Biophotonics Science and Technology, University of California, Davis, California 95616, USA

(Published 12 January 2004)

The DNA molecule, well known from biology for containing the genetic code of all living species, has recently caught the attention of chemists and physicists. A major reason for this interest is DNA's potential use in nanoelectronic devices, both as a template for assembling nanocircuits and as an element of such circuits. Without question, a truly conducting form of DNA would have a major impact on developments in nanotechnology. It has also been suggested that extended electronic states of DNA could play an important role in biology, e.g., through the processes of DNA damage sensing or repair or through long-range charge transfer. However, the electronic properties of DNA remain very controversial. Charge-transfer reactions and conductivity measurements show a large variety of possible electronic behavior, ranging from Anderson and band-gap insulators to effective molecular wires and induced superconductors. Indeed, understanding the conductance of a complicated polyelectrolytic aperiodic system is by itself a major scientific problem. In this Colloquium, the authors summarize the wide-ranging experimental and theoretical results and look for any consistencies between them. They also pose simple questions regarding the electronic states of DNA within the framework of generalized Hückel and Slater-Koster theories. The Colloquium provides a quantitative overview of DNA's electronic states as obtained from density-functional theory, focusing on dependence on structure, on molecular stretching and twisting, and on water and counterions. While there is no clear theoretical basis for truly metallic DNA, situations are discussed in which very small energy gaps might arise in the overall DNA/water/counterion complex, leading to thermally activated conduction at room temperature.

CONTENTS

I. INTRODUCTION

Half a century after the discovery of the DNA structure as reported by Watson and Crick (1953), celebrations of this important molecule abound. The principal story of DNA has long centered on the fundamental role this molecule plays in carrying the genetic code of organisms. However, there has been an upwelling of recent interest in its electronic properties, motivated by both biological and technological concerns. The highly specific binding between single strands of DNA, its related self-assembly property, and the ability to synthesize DNA in whatever sequence you want (versus the hit and miss control over, say, carbon nanotubes) have made it a suitable candidate for use in molecular electronics. Motivated by these potential applications, numerous studies of charge transport in DNA have been carried out. However, although some consensus on the dominant mechanisms of single-electron transfer in DNA seems to be emerging [see the recent review by Dekker and Ratner (2001)], the nature of DNA's intrinsic conductance properties remains highly controversial.

A. Why think of DNA as an electronic material?

As early as 1962, Eley and Spivey suggested that the interbase hybridization of π_z orbitals perpendicular to the planes of the stacked base pairs in double-stranded DNA [with the DNA helical axis parallel to the z coordinate axis, as in Fig. 1(a)] could lead to conducting behavior (Eley and Spivey, 1962). There are similar stacked aromatic crystals that are indeed metallic (Roth, 1995). The most famous of such materials are the Bechgaard salts, e.g., $(TMTSF)_2PF_6$ (Fig. 2). How-

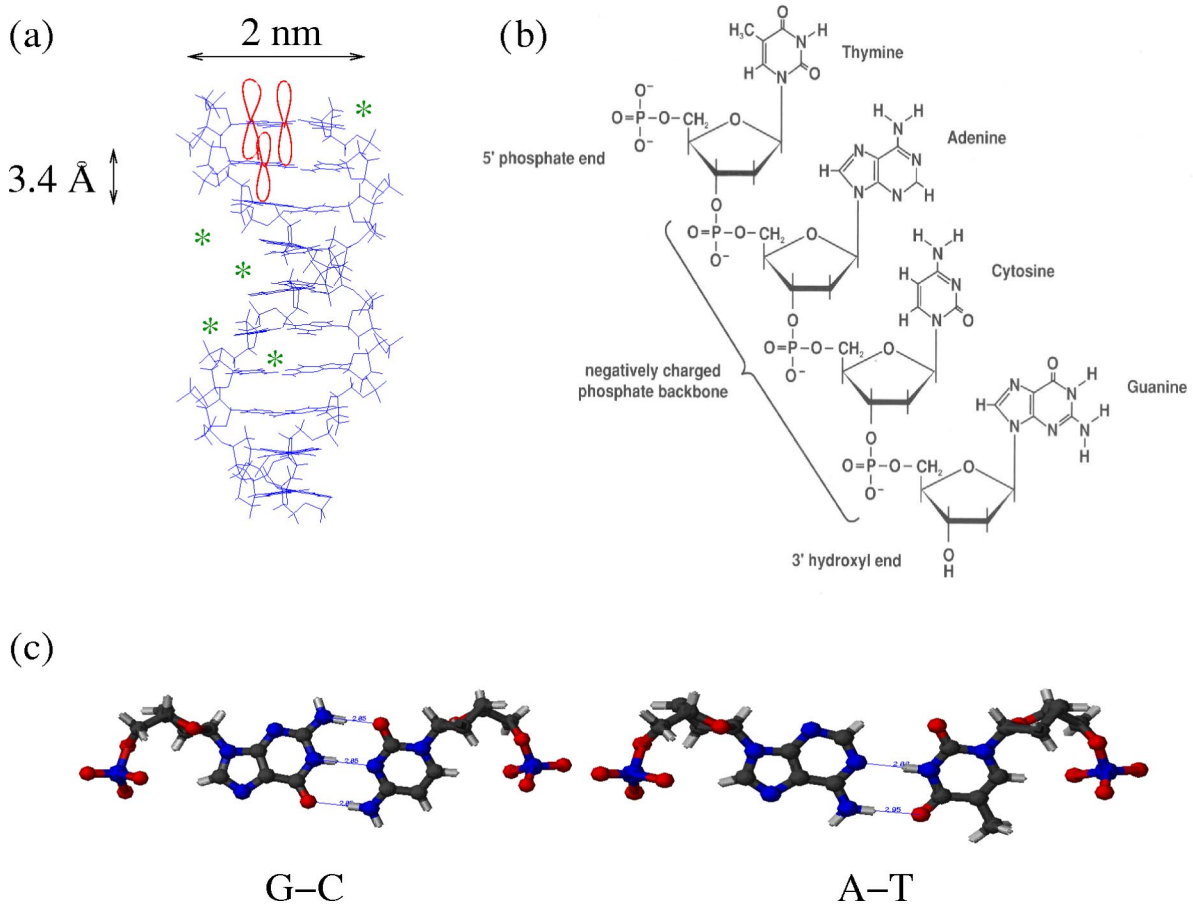

FIG. 1. (Color in online edition) Introduction to DNA structure: (a) the double helix with its stacked base pairs in the core region. A few atomic p_z orbitals (vertical loops) and positive counterions (stars) are also shown. The counterions neutralize the negatively charged phosphate groups of DNA. (b) Detailed picture of the backbone (phosphate and sugars) and the four bases. The two strands of double helical DNA have opposite directions, one going from the 5′ end to the 3′ end, the other from the 3′ end to the 5′ end. The numbers 3′ and 5′ refer to the positions of carbon in deoxyribose. From Sinden, 1994. (c) Close-up of the two possible base pairs, including sugars and phosphates: guanine (G) paired with cytosine (C) by three hydrogen bonds; adenine (A) paired with thymine (T) by two hydrogen bonds. Figures (a) and (c) prepared with the program MOLMOL (Koradi *et al.*, 1996).

ever, DNA also has important differences from these and conventional conductors. Most significantly, unlike crystals, biological DNA is not a periodic system. The largest ionization potential difference between two isolated bases is about 0.6 eV between guanine and thymine, which exceeds the estimated electronic coupling between highest occupied or lowest unoccupied molecular orbitals of neighboring base pairs. This would lead to the expectation of Anderson localization of the electronic states in the base pair stack. [However, it has recently been suggested that DNA's sequence is not truly random, but instead may show long-range correlations (Carpena *et al.*, 2002).]

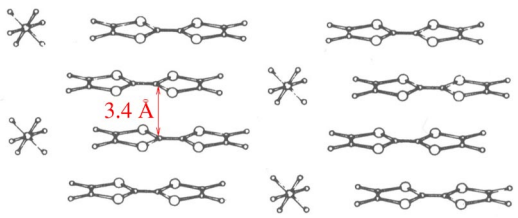

FIG. 2. (Color in online edition) The Bechgaard salt $(TMTSF)_2PF_6$—a conducting aromatic crystal. From Roth, 1995.

In addition, the double helix of DNA acts to keep the hydrophobic bases out of water, and the acidity of DNA (negative phosphate groups on the backbone) requires a proximate condensation of positively charged counterions (normally sodium or magnesium) in the environment. The water molecules and counterions are, of course, liquid, and exert non-negligible forces on the electrons in the base pair stack, which again contributes to an apparent random electronic environment. Hence it is insufficient to consider simply the molecule itself; one must also consider its surroundings.

Further complicating the study of DNA as an electronic material is the strong influence of molecular vibrations. In particular, the root-mean-square vibrational displacement of a base pair in DNA at room temperature is estimated to be about 0.3–0.4 Å (Young *et al.*, 1997), which is a tenth of the lattice constant and an order of magnitude higher than in crystals at room tem-

perature. In effect, DNA is on the verge of melting, which of course is biologically useful in terms of facilitating replication or partial uncoiling (for genetic expression, regulation, or repair), but is technologically problematic, since one would prefer a more stable material! Taken together, these structural, environmental, and vibrational properties make DNA a highly dynamic and complex system, and it is interesting to ask whether traditional concepts borrowed from solid-state physics might apply in understanding the diverse experimental results on this system.

B. DNA: A molecular wire in biological systems?

Despite the odds against a role for electronic conduction in DNA, intriguing hints of interesting electronic behavior in DNA first began to emerge a decade ago in the studies of Barton and co-workers, who observed evidence for essentially distance-independent charge transfer between DNA-intercalated transition-metal complexes (Murphy *et al.*, 1993) and noted that this could have large implications in biology and biotechnology. For instance, Barton and colleagues demonstrated photoinduced oxidation by a rhodium metallointercalator in DNA over 40 Å away within a tenth of a nanosecond (Hall *et al.*, 1996). In another experiment, a known DNA defect, the thymine dimer, could be healed from 16 base pairs away by a photoexcited rhodium intercalator molecule (Dandliker *et al.*, 1997). Moreover, this group has shown that deliberately induced damage to DNA molecules can significantly reduce electron migration, as measured through electrochemical methods (Kelley *et al.*, 1999).

These experiments on DNA in nonbiological model situations generated a number of very interesting hypotheses. For example, while a number of the proteins involved in repairing DNA damage have been identified, far less is known about the mechanism for sensing the damaged bases, which are most frequently damaged by oxidation from intracellular chemistry or extracellular ionizing radiation directly attacking the DNA or generating oxidizing adducts (new chemical species made from two separate molecular entities by changing the connectivity of their atoms but without loss of atoms); replication errors are common but less frequent by orders of magnitude (Rajski *et al.*, 2000).

While sensing during transcription or replication of DNA is currently carried out, little is known about nontranscription coupled global damage-sensing mechanisms (Friedberg, 2003). For example, while ATM phosphorylation with subsequent branching to repair or apoptosis is in some way initiated by double-strand breaks, the mechanism underlying this process is only dimly grasped (Bakknist and Kastan, 2003). It is possible that sensing involves proteins moving along the DNA and contacting the damaged region, but this is likely to be a very slow process along the 2 m of DNA in the human genome, for example.

Barton and co-workers have hypothesized that there might be signal and receiver proteins exploiting the long-range electron migration properties of DNA identified earlier. In the absence of damage, long stretches of DNA can be probed electronically, with the receiver protein reduced and detached by the transfer (oxidized receivers can reattach downstream). If a damaged region intervenes between the transmitter and receiver, the transmitter will simply move down the DNA until it hits the damaged spot, which it then "marks" for repair (Rajski *et al.*, 2000). It should be noted here that while true electron transfer can be rapid (picoseconds to nanoseconds), very-long-ranged electron migration may correspond to multiple hops and be substantially slower. However, since cell replication in a complex organism takes about a day, even a slowdown by several orders of magnitude is not a problem.

Another intriguing idea is that guanine-rich regions of DNA serve as "cathodic" protectors (Heller, 2000). Since guanine (and especially sequences of guanine) has the smallest oxidation potential compared to the other bases, long-range charge transfer of holes to short guanine-rich overhang regions at the termini of chromosomes could protect DNA from oxidative stress.

C. DNA: A building block in molecular electronics?

In the mid 1990s, shortly after Barton's molecular wire hypothesis, Warman *et al.* (1996) measured the radiation-induced conductivity of aligned DNA films. Although hydrated DNA showed mobile charge carriers, the lack of anisotropy in the conductivity argued against a quasi-one-dimensional metal.

For the last few years there have been many new experimental studies of DNA's conductance, leading to a variety of results. These have ranged from wide-gap insulating behavior to proximity-induced superconductivity. It is of immense importance to resolve these issues, especially since conducting DNA could have a variety of applications in molecular electronics and biotechnology. Just to name some potential applications, consider the DNA chip, which is used for DNA sequencing, disease screening, and gene expression analysis. If DNA can conduct sufficiently well, a sequence could be read out electronically instead of visually (using fluorescent dyes) as is done currently. The idea is that floppy single strands of DNA are insulating, but well-stacked double-stranded DNA after successful hybridization could be conducting, thus allowing an electronic readout. This approach may have the advantage of a higher density of single-strand DNA samples on the chip (the density of single-strand regions on optically read chips right now is resolution limited) with the potential for a faster and more efficient sequence analysis.

DNA's sequence-dependent self-assembly property can be used to build complex nanowire geometrical arrangements. Interesting topological structures (e.g., cubes) have indeed been created with DNA by Seeman and co-workers (Chen and Seeman, 1991; Zhang and Seeman, 1994). DNA-based templating may find important applications in nanoelectronics even if DNA itself is insulating. For example, the "sticky ends" (single-

stranded overhang regions at the ends of the helix) can be used to attach single DNA molecules to modified metal electrodes (gluing technique; Braun *et al.*, 1998; Rakitin *et al.*, 2001). Indeed, Braun *et al.* (1998) were able to successfully coat DNA with silver to obtain thin metallic wires. Rakitin *et al.* (2001) made DNA metallic by exchanging protons for doubly positive zinc ions inside the helix at a high *p*H value. Finally, in the spirit of scaling down solid-state devices to nanosize, the first single-DNA field-effect transistor was built by Kawai's group (Yoo *et al.*, 2001). The latter does use the intrinsic conducting properties of short DNA segments.

D. Overview of this Colloquium

The purpose of this colloquium is to review the diverse previous experimental and theoretical efforts to understand the electronic properties of DNA and to look for common threads. Furthermore, we summarize and elucidate basic aspects of DNA electronics in terms of generalized Hückel and Slater-Koster theories involving its π orbitals. We also discuss more quantitatively the effects of DNA structure and environment on its molecular states and conductivity, using a density-functional-based electronic structure program, SIESTA.

This Colloquium is structured as follows. Section II introduces the main concepts, starting from the similarity of DNA and conducting aromatic crystals. It then explains the competition between $pp\sigma$ and $pp\pi$ binding, which determines whether the aromatic π stack is metallic or insulating. It ends with the effects of vibrations on the electronic coupling between DNA's basic units, its base pairs. In Sec. III we summarize the various conductivity measurements and stress that the experimental conditions are as different as the outcomes. We discuss ways to reconcile some of the conflicting results.

Computational approaches to the study of DNA have been limited due to its large unit cell. In Sec. IV previous theoretical efforts and *ab initio* calculations are reviewed. Section V summarizes efforts to apply the concepts developed in Sec. II to look at the role of DNA's structure (A-DNA or dried biological DNA, B-DNA or wet biological DNA, S-DNA or stretched biological DNA) in π coupling between base pairs. We then consider whether solvent and counterions can produce impurity states in the π-π^* energy gap of DNA and/or lead to doping. The effects of different structures on the π overlap are discussed using elementary Hückel theory with a Slater-Koster parametrization of interatomic matrix elements. The effects of solvent and counterions (sodium and magnesium) are discussed based on density-functional theory (DFT) calculations using the program SIESTA and lead to some interesting doping scenarios (Endres *et al.*, 2002). We finally present our conclusions in Sec. VI.

II. BASIC CONCEPTS

A. The π-π electronic coupling

Shortly after the discovery of DNA's double-helix structure by Watson and Crick (1953), Eley and Spivey (1962) suggested that π-π interactions of stacked base pairs in double-stranded DNA could lead to conducting behavior. The reasoning behind this idea was that DNA's bases are aromatic entities (i.e., organic compounds containing planar, unsaturated, benzene-type ring structures) whose atomic p_z orbitals perpendicular to the plane of the base can form rather delocalized π bonding and π^* antibonding orbitals. These are separated by an energy gap of about 4 eV (Helgren *et al.*, 2002). If the coupling between the base pairs is strong enough, this could lead to extended states along the helical axis with a reduced DNA energy gap, due to level broadening. For a vanishing gap this could possibly lead to metallic DNA. On the other hand, even in the case of a nonvanishing gap, there is still the possibility of doping by either electrons or holes, in analogy to conventional doped semiconductors. Figure 1(a) shows a typical DNA structure in which some atomic p_z orbitals are indicated by vertical lobes. Part (b) shows the negatively charged backbone in more detail, while part (c) shows the two possible base pair combinations, guanine (G) paired with cytosine (C) and adenine (A) paired with thymine (T).

There are other stacked aromatic crystals that are indeed metallic (Roth, 1995). Figure 2 shows $(TMTSF)_2PF_6$—a so-called Bechgaard salt. The stacked organic donors transfer electrons to inorganic acceptors (e.g., PF_6). This results in partially filled metallic π bands. At low temperature, some of these systems become superconducting, while others undergo a metal-to-insulator transition by the Peierls mechanism.

In order to have extended, metallic states in DNA, the π and π^* states of the base pairs have to overlap sufficiently. This depends again on the twist angle and the separation of two successive base pairs. Since the π and π^* orbitals are formed by the atomic p_z orbitals perpendicular to the base pairs and pointing along the helical axis, one can also consider a simple Hückel model using just these (Endres *et al.*, 2002). Two p_z orbitals from different base pairs, as shown in Fig. 3, couple by $pp\sigma$ and $pp\pi$ hybridization. These hybridization matrix elements have different signs due to the signs of the lobes of the p_z orbitals and may be modeled with the semiempirical Slater-Koster theory (Slater and Koster, 1954; Harrison, 1989),

$$V_{ppX} = \eta_{ppX} \frac{\hbar^2}{md^2} e^{-d/R_c} \tag{1}$$

where $\eta_{pp\sigma} > 0$ and $\eta_{pp\pi} < 0$. In Slater-Koster theory d and m are the distance between the orbitals (see Fig. 3) and electron mass, and $\hbar^2/m = 7.62$ eV Å^2. The exponential distance cutoff R_c is additionally introduced to describe the exponential tails of the wave functions at large separations. The parameters η and R_c can be determined by matching to results of *ab initio* calculations.

The interatomic electron transfer matrix element between two "parallel" p_z orbitals on neighboring base pairs is then a combination of $pp\sigma$ and $pp\pi$ hybridization, which are given by

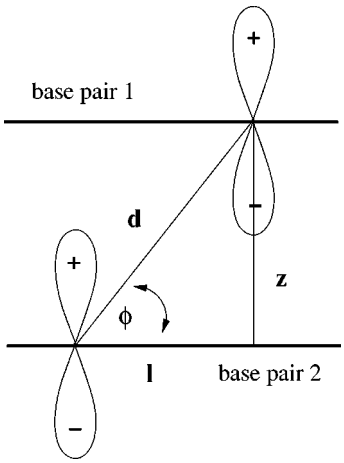

FIG. 3. The coupling between two atomic p_z orbitals from parallel base pairs. The $pp\sigma$ and $pp\pi$ contributions have opposite signs and can cancel each other. Here, d and l are the distance between the two orbitals and its projection on either base pair plane, respectively, and z is the separation of the two base pairs.

$$V=\sin^2\phi V_{pp\sigma}+\cos^2\phi V_{pp\pi}$$
$$=\frac{\hbar^2 e^{-d/R_c}}{md^2}\left[(\eta_{pp\sigma}+|\eta_{pp\pi}|)\frac{z^2}{l^2+z^2}-|\eta_{pp\pi}|\right], \quad (2)$$

where l and z are defined in Fig. 3. According to this formula, complete annihilation of V occurs when

$$\frac{l}{z}=\sqrt{\frac{\eta_{pp\sigma}}{|\eta_{pp\pi}|}}\approx 2.0. \quad (3)$$

Here, the value 2.0 on right-hand side follows from a fit (Endres *et al.*, 2002), and z is about 3.4 Å for both A- and B-DNA Hence, for a fixed base pair separation z, poor contacts between two atomic orbitals of adjacent base pairs reduce their electronic coupling contribution to the total electronic coupling between molecular orbitals on neighboring base pairs. (A good contact is defined by $l\approx 0$ Å.) The electronic coupling between base pairs can be reduced for two reasons. First, the positive $pp\sigma$ and negative $pp\pi$ interaction between two interacting atomic p_z orbitals can reduce or almost cancel each other, leading to a small net atomic pair interaction. Second, some rather large, predominantly σ and π pair interactions can reduce or cancel each other when added up to calculate the total base pair coupling. In other words, small base pair coupling can be caused by small individual atomic pair interactions or by an equal number of rather large positive and negative ones. This cancellation tendency is particularly important for A-DNA.

The resulting couplings exceed 1 eV for the p_z orbitals that are right on top of each other. But the actual couplings between base pairs are given by the overlap of the π or π^* orbitals, which are extended in the plane of the base pair, and these are generally much smaller. In other words, the participation ratio for each single p_z orbital in the overall base pair molecular orbital is small. Approximating the molecular orbitals of different base pairs as being orthogonal to each other, one can describe the coupling between two successive base pairs by

$$t^{n,m}=\sum_i^{N_1}\sum_j^{N_2} V_{ij}^{12} c_i^{1,n} c_j^{2,m}. \quad (4)$$

Here i and j run over the N_1 and N_2 p_z orbitals of base pairs 1 and 2, respectively. G-C has 19 while A-T has only 18 p_z orbitals. The $c_i^{1,n}$ is the ith LCAO (linear combination of atomic orbitals) coefficient of the nth molecular orbital of base pair 1. V is the off-diagonal block matrix $(N_1\times N_2)$ of the Hamiltonian matrix $(N_1+N_2)\times(N_1+N_2)$ describing the interaction between the states of the two base pairs. Hence according to Eq. (4) each interaction matrix element connecting two atomic p_z orbitals from different base pairs is multiplied by two LCAO coefficients, whose product has a magnitude of order 1/10. Hence each hybridization matrix element has only a small contribution to the inter-base-pair electronic coupling $t^{n,m}$. As one can see from Eq. (2), the coupling $t^{n,m}$ will depend on how well the base pairs are stacked, i.e., on their relative twist angle and their separation. These variables are determined by the DNA structure, i.e., A-, B-, or S-DNA. This is discussed in more detail in Sec. V. On the other hand, the dependence of $t^{n,m}$ on these variables is also important to understand, since at finite temperature the base pairs of DNA will oscillate about their equilibrium positions. This can affect the electronic coupling and hence the charge-transfer rate and conductivity.

B. Coupling to vibrations

In this section we discuss the effects of torsional modes on the electronic coupling $t^{n,m}$ by examining results from a DFT calculation. On general grounds one would expect the single electron or hole transfer to be very sensitive to the motion of base pairs. One experiment finds two different time scales (5 and 75 ps) in charge-transfer experiments (Wan *et al.*, 1999). The longer-time items presumably stem from a necessary reorientation of base pairs in order to make charge transfer possible (Wan *et al.*, 1999; Bruinsma *et al.*, 2000). This is consistent with the extremely soft torsional acoustic modes ($\leqslant 20$ cm^{-1}) calculated theoretically (Cocco and Monasson, 2000) and also seen in the dynamic Stokes shifts in fluorescence spectra (Brauns *et al.*, 1999).

In Fig. 4 we show the electronic coupling $t^{n,m}$ computed from DFT as a function of the twist angle about the helical axis. Note that we measure the twist relative to the equilibrium value of 36° for biological B-DNA, which has a canonical equilibrium base pair separation of $z=3.4$ Å (Chandrasekaran and Arnott, 1996). We disregard the influence of sequence upon base pair separation and relative twist here (Breslauer *et al.*, 1986; Gorin *et al.*, 1995; Olson and Zhurkin, 2000).

The different plots correspond to couplings between HOMO's (highest occupied molecular orbital, with energy corresponding to the ionization energy) and LUMO's (lowest unoccupied molecular orbital, with en-

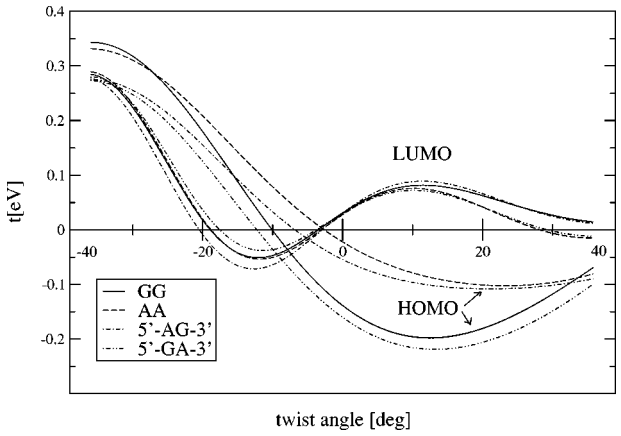

FIG. 4. Change of electronic coupling t between frontier orbitals (HOMO's and LUMO's) of two base pairs with a relative twist angle about the equilibrium angle 36° (set to zero). The base pair separation is kept fixed at $z=3.4$ Å. The different plots correspond to various base pair dimers (two-base-pair-long DNA), e.g., sequences GG, AA, AG, GA counted from the 5′ end to the 3′ end.

ergy corresponding to the electron affinity energy) between different base pair dimers. The coupling between HOMO's is important for hole transport, while the coupling between LUMO's is important for electron transport.

According to Fig. 4 there are sign changes of $t^{n,m}$ as a function of the twist angle. Interestingly, the sign changes occur near the equilibrium twist angle of A-DNA. The LCAO coefficients stay approximately constant during the rotation, so that the sign changes must stem from the interaction matrix elements V_{ij}^{12}, which depend strongly on the geometry of the base pair dimer. At ambient temperatures, the twist angle has a standard deviation of about 8° (Young *et al.*, 1997). In the interval $(-8°;+8°)$ it is possible that $t^{n,m}$ vanishes. One can easily imagine that base pair to base pair charge transport is limited by the low twisting frequencies, of order 10^{11}–10^{12} Hz, particularly in structures close to the A form. Separately at an angle of $-36°$, the base pairs are perfectly aligned (for identical base pairs) and parallel to each other. This leads to optimal σ overlap and to a maximal $t^{n,m}$. At least for identical base pairs this can easily be rationalized, since we get approximately $t \approx \Sigma_i^N V_{ii}(c_i)^2 > 0$, where V_{ii} are all positive due to σ overlap and add up to give a large contribution. [Note that V_{ij} with $i \neq j$ are typically very small; note also that for simplicity we have omitted here the superscripts to the coefficients c_i that appear in Eq. (4).]

The dependence of $t^{n,m}$ on the base pair separation is less dramatic and is discussed elsewhere (Endres *et al.*, 2002).

III. EXPERIMENTAL OVERVIEW

A. Charge transfer

Hole transfer reactions in DNA have been studied by Henderson *et al.* (1999), Lewis *et al.* (2000), Giese *et al.* (2001), and others. Initially, DNA is doped (in chemical terminology, oxidized or reduced). The base guanine is an easy target for many oxidizing agents. A hole placed in a guanine's HOMO is only about 0.2 eV above the next lower occupied orbitals (of adenine; thymine and cytosine are even lower; Bixon and Jortner, 2001a) and can begin to migrate through the DNA to find other easily oxidizable sites, like other guanines or sequences of guanines. In this scenario of hole transport DNA's LUMO is not involved, because it is about 4 eV higher in energy. The charge-migration mechanism can involve a single quantum-mechanical tunneling event at short distances, a phenomenon first described quantitatively by the celebrated theory of Marcus (1956a, 1956b, 1993, 1998). Alternatively, charge transfer can involve several direction-uncorrelated tunneling events displaying a one-dimensional random walk. A more detailed introduction to the theory of charge transfer is given in Sec. IV. Put simply, the picture that emerges from experiments (Dekker and Ratner, 2001) is that superexchange (tunneling) occurs between guanines (or guanine dimers and trimers) separated by three or fewer A-T base pairs, while for larger separations diffusive hopping dominates the transfer. Some of the pioneering work by Barton, Zewail, Wan, and co-workers on photoinduced charge transfer shows a weak distance dependence (Murphy *et al.*, 1993; Wan *et al.*, 1999), which led to suggestions that DNA could act as a "molecular wire." However, later work using different donors and acceptors argued against the wirelike picture for DNA (Wan *et al.*, 2000). (We note that the use of the term "wire" in the DNA charge-transfer literature is somewhat problematic, if not wholly ill defined. In this context we take "wire" to mean that injected holes or electrons can enjoy long-range transport, i.e., over tens of angstroms, on fast time scales of picoseconds or less.) The interpretation of some of these experiments may be even more uncertain, since it is not even clear if the reaction involves electron or hole transfer.

B. Conductivity

The question of whether DNA is intrinsically conducting is an unsolved problem. The experimental outcomes are amazingly different, covering all possible results: insulating (Braun *et al.*, 1998; de Pablo *et al.*, 2000; Storm *et al.*, 2001; Zhang *et al.*, 2002), semiconducting (Porath *et al.*, 2000), Ohmic (Fink and Schönenberger, 1999; Cai *et al.*, 2000; Tran *et al.*, 2000; Rakitin *et al.*, 2001; Yoo *et al.*, 2001), and even induced superconductivity (Kasumov *et al.*, 2001). One difficulty is to make cleanly reproducible and easily interpreted experiments with nanoscale dimensions. The other difficulties have to do with the large number of "variables" (experimental conditions) on which the outcome of the experiments depend. Furthermore, experimental results are often presented in short-format letter journals condensing the description of experimental conditions and protocols. This makes it hard for one to judge the quality of the experi-

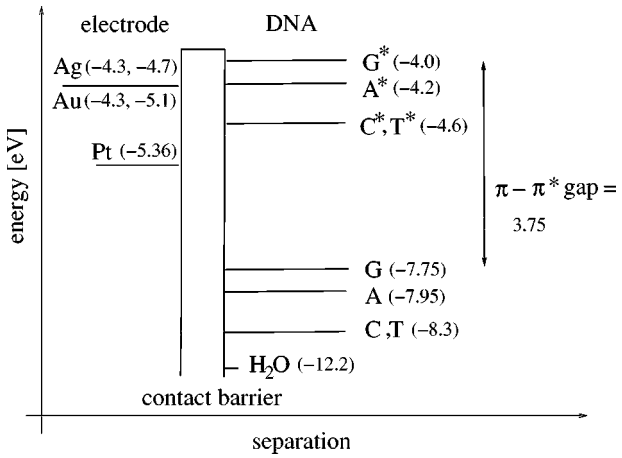

FIG. 5. Schematics of metal work functions and DNA energy levels at an electrode/DNA junction. The values of the metal work functions and the first ionization potential of gaseous water are taken from Hodgman and Veazey (1966), Ashcroft and Mermin (1976), the website http://kasap3.usask.ca/server/kasap/Tables/Metal1.html, and Barrow (1988). The value of water is expected to change drastically in the proximity of charged DNA and counterions. The DNA gap of 3.75 eV is taken from an optical absorption measurement, which also corresponds to the excitation energies of single bases (Helgren *et al.*, 2002). The excited-state energies of the bases are obtained from the single-base ionization energies by simply adding the gap size. The ionization energies are a tricky business: according to Koopmans's theorem the ionization energies correspond to the HOMO energies obtained from a Hartree-Fock *ab initio* method. The guanine (G) value is taken from Sugiyama and Saito (1996) and Wetmore *et al.* (2000), which is close to the experimental value of guanine in the gas phase (Orlov *et al.*, 1976; Lias *et al.*, 1988). The values for adenine (A), thymine (T), and cytosine (C) are not taken from an *ab initio* calculation or experiment of single bases, since they may be too negative relative to G in a DNA environment. From analyzing yield data of charge transfer in DNA (Bixon and Jortner, 2001a), they are likely to be closer to G than isolated bases in the gas phase (Orlov *et al.*, 1976; Lias *et al.*, 1988) or solution (Seidel *et al.*, 1996; Steenken and Jovanovic, 1997).

ments and relate them to one another. Of course, in this Colloquium we can only comment upon the details presented in the literature.

Assuming that the literature data are not artifacts and provide useful information about DNA conductivity, we can separate the sources of experimental uncertainties into two categories:

- *Contacts between the electrode and the DNA molecule*: The contact is characterized by the work function of the electrode, as well as the nature of the tunneling barrier. Is there direct metal-π orbital contact or do charge carriers first have to tunnel through the backbone? If so, what is the size of the barrier? Unfortunately, only the work functions of metal electrodes are more or less known. In the important case of gold, it is not even clear if the Au work function is below or above the DNA LUMO (Fig. 5). [Electron affinity measurements of single bases in the gas phase suggest that the Au work function is below (Aflatooni *et al.*, 1998).]
- *Differences in the DNA molecules and their environments*:
  There are many factors that influence DNA conductivity:

(1) DNA sequence. Figure 5 shows estimates of metal work functions and ionization potentials of bases. Since each base has its own molecular energy level, a nonperiodic sequence will lead to disorder along the one-dimensional molecule.
(2) Length of the DNA molecule.
(3) Character of the DNA molecule (e.g., ropes vs single molecules).
(4) Environment of DNA (influence of water and counterions). Here, for example, the number of water molecules is critical in influencing structure: for five to ten water molecules per base the A-DNA structure obtains, while for >13 water molecules per base the B structure is preferred (Warman *et al.*, 1996).
(5) Microstructure of DNA (dependent upon humidity, stretching, or combing preparation conditions).
(6) Interfacial character (e.g., free-standing molecules, surface-bound DNA on, say, mica).
(7) Preparation and detection protocols [drying of DNA via flowing N_2 gas, which tends to provide two to three water molecules per nucleotide (Tran *et al.*, 2000); detection of single molecules by scanning probe microscopies or electron microscopies, which can "dope" the molecules].

Some of the above-mentioned variables are hard to control, e.g., the nature of the contact and the actual structure of DNA. Some success has recently been achieved by Hartzell *et al.* (2003a, 2003b) concerning the dependence of the conductivity on the nature of the contact to the electrode as well as on whether DNA is nicked or repaired. However, the same authors admit that, while some experimental parameters are rather well controlled, other important ones, like how many DNA molecules are actually bridging the electrodes, are not.

A key experimental challenge in measuring DNA conductance lies in the attachment of a DNA bundle or single molecule to two electrodes. This has been made possible largely due to advancements in nanotechnology. Electron-beam lithography is used to fabricate nanoelectrodes, atomic force microscopy (AFM) and low-energy electron point source (LEEPS) microscopy are used to image the sample, and scanning tunneling microscopes (STM) can be utilized to induce a tunneling current. In order to attach single DNA molecules to metal electrodes, a DNA oligomer-based[1] "gluing" technique

[1]An oligomer is a molecule comprising only a few base pair monomers.

was developed in which sticky ends of DNA (single-stranded "overhang" regions) are hybridized to short surface-bound oligomers (Braun *et al.*, 1998; Zhang *et al.*, 2002; Hartzell *et al.*, 2003a, 2003b). Similarly, DNA modified with thiol (SH) groups at the 5′ ends can directly hybridize on gold or platinum electrodes (Storm *et al.*, 2001). Another method of aligning DNA molecules between the leads is called "electrostatic trapping." An electric field between two electrodes polarizes a nearby molecule in a droplet of DNA solution, which is then attracted to the gap between the electrodes owing to the field gradient (Porath *et al.*, 2000; Cai *et al.*, 2001).

The experimental results from different groups are summarized in Table I and can be clearly seen to vary widely. Again, assuming the results not to be artifacts, we can examine them to see if they can be explained consistently owing to the large number of factors mentioned above. To do so, we divide the results into the following four classes:

- **Class 1: DNA is an insulator at room temperature,** as found by Braun *et al.* (1998), de Pablo *et al.* (2000), Storm *et al.* (2001), and Zhang *et al.* (2002). These samples show I-V characteristics with essentially no discernible conductance out to ± 10-V bias, consistent with completely localized states.
- **Class 2: DNA is a true wide-band-gap semiconductor at all temperatures,** as measured by Porath *et al.* (2000) and (for B-DNA oligomers) by Rakitin *et al.* (2001). See the inset to Fig. 2 of Rakitin *et al.* (2001).
- **Class 3: DNA is Ohmic or nearly Ohmic at room temperature** (it may show a small activation gap of less than 0.2 eV) and is insulating at low temperatures, as found in experiments by Fink and Schönenberger (1999), Cai *et al.* (2000), Tran *et al.* (2000), Rakitin *et al.* (2001) (dried B-DNA droplets, as shown in Fig. 2 of this reference), Yoo *et al.* (2001), and Hartzell *et al.* (2003a, 2003b).
- **Class 4: DNA is truly metallic down to low temperatures** requiring extended molecular energy bands, as suggested by Kasumov *et al.* (2001). This isolated case is the hardest to account for. Since, to our knowledge, there has been no independent verification of this result, it is the least reliable one.

Consider first the experiments in class 1. Braun and co-workers used μm long λ-DNA, whose 3′ ends were chemically anchored to Au electrodes through sulfur-gold interactions. This very elegant technique, observed by fluorescence spectroscopy, produced single, free-hanging DNA molecules between the electrodes. They measured no current between -10- and 10-V bias voltage. This result was confirmed by Pablo and co-workers, who could not get any current flowing through a SFM tip and a gold electrode connected by λ-DNA sitting on an insulating mica surface. Since biological λ-DNA has a nonperiodic base pair sequence, its mixed sequence could result in static disorder and subsequent localization of molecular orbitals.

Motivated by this, Storm and co-workers performed extensive measurements, varying the sequence of DNA [using λ-DNA, as well as synthetic poly(G)-poly(C) DNA]. In addition, they also varied the type of electrode (Pt and Au) and the insulating surface (SiO_2, mica) on which the molecules sat. They also measured zero conductance. However, on their AFM images of the sample, the height of DNA lying on the insulating surface was only 0.5 nm. Since a DNA double helix has a diameter of about 2 nm, this indicates that (perhaps due to weak binding to the surface) the sample no longer contained well-stacked base pairs with base pair separation of about 3.4 Å. This was confirmed by Cai and co-workers, whose DNA on mica, elongated with the free-flowing method, had an increased helical periodicity ($\sim$7.2 Å; Cai *et al.*, 2001). Very recent experiments by Zhang and co-workers displayed similar insulating behavior at bias potentials up to 20 V. In their experiment, a few DNA molecules were stretched by a buffer flow across the gold electrodes, where they were anchored covalently (Zhang *et al.*, 2002).

In class 2 there are two experiments which show wide-band-gap semiconductor behavior. This is what one might expect for short DNA molecules assuming that the bases of DNA have a rather large HOMO-LUMO gap ($\sim$4 eV) with the metal work functions sitting inside the gap. In the experiment by Porath *et al.* (2000), a single short (30 base pairs) DNA molecule, or at most a few, with a homogeneous sequence [poly(G)-poly(C)], free-hanging between two Pt electrodes, was measured and imaged with a scanning electron microscope. This experiment is remarkable in the sense that it is the only one with a sample that is only a few base pairs long. Given the persistence length of double-stranded DNA (about 100 base pairs at room temperature), such samples are plausibly free of the kinks and defects in the molecule that would lead to extra uncertainty and interruption of the π-π interactions. Hence the result is expected to be rather reliable. The bias voltage gap is of order 1–2 eV, which can probably be interpreted as the energy difference between the Pt work function (-5.36 eV) and either the guanine HOMO (G; ~ -7.75 eV; Berlin *et al.*, 2000) or the cytosine LUMO (C^*; ~ -4.6 eV)—whichever is closer to the Pt work function in reality. The differential conductance in such experiments can sample the density of electronic states. Given the reproducible and relatively sharp peaks observed for a given trapped molecule, Porath *et al.* (2000) concluded that this was reasonable evidence for the existence of coherent electronic states extended across the DNA molecule.

Hence it seems that short, homogeneous DNA molecules are wide-band-gap semiconductors. The measured strong temperature dependence of the gap Δ ($|d\Delta/dT| \approx 1-2$ eV/300 K) is, on the other hand, not easily explainable within the coherent energy-band picture (Hjort and Strafström, 2001). Moreover, Rakitin and co-workers measured a very similar bias voltage gap, although they worked with Au electrodes with a higher work function (-5.1 to -4.3 eV). The sample

TABLE I. Overview of recent conductivity measurements of DNA. Four classes, labeled 1–4, of different experimental outcomes can be identified, although this classification is by no means unique. Notation: RT = room temperature.

Class	Group	DNA sample[a]	Result	Electrodes	Method	Ions[b]
1. Anderson insulator	Storm *et al.* (2001)	single λ-DNA/polyG-polyC	insulating (at RT) (DNA height: 0.5 nm)	Pt/Au	on SiO_2, mica surface	Mg^{2+}
	Braun *et al.* (1998)[c]	single λ-DNA	insulating (at RT)	Au	free hanging (gluing technique)	Na^+
	Zhang *et al.* (2002)					?
	de Pablo *et al.* (2000)		(conducting if doped)		SFM, on mica	
2. Band-gap insulator	Porath *et al.* (2000)	single polyG-polyC (only 30 bps)	wide band-gap semiconductor (at all RT)	Pt	free hanging	Na^+
	Rakitin *et al.* (2001)[d]	single, short oligomer-λ-DNA	(at RT)	Au	(gluing technique)	
3. Activated hopping conductor	Rakitin *et al.* (2001)	bundles of λ-DNA	narrow "band-gap" semiconductor (at RT)	Au	free hanging	Na^+
	Yoo *et al.* (2001)	supercoiled polyG-polyC polyA-polyT	linear Ohmic at RT insulating at low T	Au/Ti	on SiO_2	
	Cai *et al.* (2000)	networks of bundles polyG-polyC/polyA-polyT	linear Ohmic (at RT)	Au	SFM, on mica	
	Tran *et al.* (2000)	supercoiled dry and wet λ-DNA	hopping conductivity	none	microwave absorption	
	Fink and Schönenberger (1999)	bundles of λ-DNA	conducting (doped) (at RT)	Au	free hanging	
4. Conductor	Kasumov *et al.* (2001)	few λ-DNA molecules	induced superconductivity ($T<1$K)	Re/C	on mica	Mg^{2+}

[a]Except for the experiment by Porath, μm-long DNA was used. Except for Tran, solely dry DNA was measured.
[b]Predominant type of ions to the best of our knowledge. There are, of course, always protons present, depending on the *p*H value.
[c]The main goal is to use DNA as a template to grow thin silver wires.
[d]The main goal is the so-called *M*-DNA (M = Zn).

(labeled "type 3" in their notation) contained several-μm-long λ-DNA, which should be more insulating, but similar currents ($\sim$nA) were measured. This can, however, be due to large contact resistances (which are unknown and could dominate over the DNA's resistance). The short homogeneous oligomers whose sticky ends attached the λ-DNA to the electrodes by sulfur-gold bonds may conduct as poorly as the van der Waals contact in Porath's experiment. Note that both Porath's and Rakitin's experiments have samples with a few free-hanging DNA molecules in common.

In class 3 almost Ohmic conductance at room temperature was measured. These experiments were done on DNA bundles, ropes, or supercoiled DNA with possibly solvent molecules trapped in between. The stunning early result by Fink and Schönenberger (1999), who found Ohmic behavior of free-hanging λ-DNA ropes at room temperature, fueled the hope that DNA could make a good conducting wire. The DNA bundles were laid across 2-μm holes in Au-coated carbon foil, which served as one electrode. The conductance was measured with a metal-coated mechanical tip that touched the bundle and served as the second electrode. This procedure was imaged with a low-energy electron point source (LEEPS) microscope that employed coherent electrons of approximately 70 eV. As shown by de Pablo *et al.* (2000), the observed conductance may have been induced by doping effects through the imaging electrons of the microscope. Their initially insulating sample became finally conducting (Ohmic) when irradiated with a 100-eV low-energy electron beam. The resistance decreased from 10^{12} Ω to 200 MΩ (for comparison, a thin copper wire of the same radius and length has a resistance of only 200 Ω). The other experiments in class 3 by Tran *et al.* (2000), Rakitin *et al.* (2001), and Yoo *et al.* (2001) showed a small activation gap ($\leqslant$0.2 eV) at room temperature even though very different experimental setups were used.

Yoo and co-workers used μm-long poly(G)-poly(C) and poly(A)-poly(T) DNA molecules that were trapped between Au/Ti nanoelectrodes separated by 20 nm. The high-temperature activation gaps obtained were 0.12 and 0.18 eV, respectively. An activation gap of about 0.2 eV was also found by Rakitin and co-workers for 15-μm-long λ-DNA (their "type 1 sample") at room temperature. The buffer with DNA was dropped across Au electrodes and subsequently dried. AFM images of the sample indicated ropes of DNA containing roughly 300 molecules.

In a unique set of experiments Tran *et al.* (2000) measured the ac conductivity of λ-DNA from the absorption in a microwave cavity, which does not require any contacts and so provides valuable information about the DNA molecule itself. Interestingly, they could also do experiments on wet DNA in a buffer solution and over a wide temperature range. DNA in the buffer solution had approximately one order of magnitude greater conductivity than the dry form, consistent with the better base pair stacking in B form compared to A form (see also Helgren *et al.*, 2002).

More remarkable are two temperature regimes of the conductivity: above a temperature of about 200–250 K the conductivity displayed a strong temperature-dependent, activated behavior with an activation gap of approximately 0.16 eV. Below the threshold temperature, it depended only slightly on the temperature.

Tran *et al.* (2000) have speculated that the weak temperature dependence may not be electronic in nature, but instead may be caused by ionic conduction, or else by reorientation of water dipoles. Similarly, it was pointed out that the increase in the ac conductivity with humidity might be explained by an increase of single-molecule dipole relaxation losses plus collective reorientation of water clusters at strong humidity (Briman *et al.*, 2003).

Conversely, it has been suggested that these alternative mechanisms can be ruled out since the temperature-dependent dc conductance at zero bias voltage found by Yoo and co-workers shows two very similar temperature regimes. Concerning the increase of the ac conductance with humidity, similar experiments on frozen DNA samples with immobilized water molecules and counterions show a similar dependence of the conductivity on humidity (Warman *et al.*, 1996). However under such physical conditions reorientation of water dipoles seems unlikely.

The temperature dependence in several experiments can be explained by the variable-range-hopping mechanism (Yu and Song, 2000) or the small-polaron model (Yoo *et al.*, 2001). Although one has some idea about the conduction mechanism, neither the nature of small activation gaps nor the origin of free charge carriers is yet clear. Without something like doping or finding states not associated with the base pair stack, it is unlikely that the small activation gap can be accounted for.

In class 4 a single experiment by Kasumov and co-workers showed resistance data consistent with induced superconductivity in DNA. In their experiment 16-μm-long λ-DNA was metallic down to extremely low temperatures requiring true extended states. Initially the DNA was combed by the buffer flow and may have touched the insulating but charged mica between the electrodes. This experiment differs from all others in that a buffer with predominantly divalent magnesium counterions was used. (Whether this choice could lead to doping of the DNA molecules will be explored in Sec. V.B.)

At temperatures below 1 K the rhenium electrodes became superconducting and the proximity effect was observed in some samples in which a few DNA molecules were observed to span the electrodes. The existence of molecules across the electrode gap was confirmed with *nondoping* atomic force microscopy, and the resistance of the best samples was at the quantum wire limit of $h/2e^2 = 12.9$ kΩ (Anderson, 1958; Thouless, 1977). This resistance value is of fundamental importance. If the intrinsic resistance of a thin wire at $T = 0$ is larger than the resistance quantum, it cannot be considered a true metal. However, since the contact resistance is unknown, it is hard to determine the intrinsic resis-

tance of a thin wire or molecule. The resistance obtained by Porath and co-workers (short homogeneous sequence) is about 3 GΩ at a bias voltage of 4 V. This is much larger than the above maximum metallic resistance for thin wires, but how much is due to the contacts?

One indication that DNA's resistance is above the maximum metallic value, the resistance quantum, stems from the experimental fact that DNA displays excess resistance, i.e., the resistance increases exponentially with the length of the wire instead of linearly, as is common for Ohmic materials. The data were provided by Cai *et al.* (2000) and taken from self-assembled DNA networks.

The question remains, however, what is the origin of the near-Ohmic behavior found in bundles, networks of bundles, or supercoiled samples? Does it stem from the possible stabilization of floppy single DNA molecules by the bundles, or do condensed water and counterions trapped between the DNA molecules lead to a different pathway for charge transport than through π stacked base pairs? If so, this could explain the lack of anisotropy of conductance seen in films of oriented DNA molecules (Warman *et al.*, 1996), or as intrinsically present in supercoiled DNA samples (Cai *et al.*, 2000; Tran *et al.*, 2000; Yoo *et al.*, 2001). There seems to be a weak sequence dependence, however, arguing in favor of a one-dimensional pathway through stacked base pairs. Poly(G)-poly(C) and poly(A)-poly(T) samples showed slightly different activation gaps (Yoo *et al.*, 2001). This, however, could also be due to the fact that (at least crystalline) poly(G)-poly(C) and poly(A)-poly(T) DNA have different helical rises, 2.88 and 3.22 Å, respectively, which may have caused condensed water and counterions to form different patterns. It is also interesting to note the somewhat larger conductivity for wet compared to dry DNA, but both dry and wet have the same activation gap ($\sim$0.16 eV), as inferred from contactless measurements in a microwave cavity (Tran *et al.*, 2000). The dependence of the conductance on humidity could have to do with the more regular structure of DNA at high humidity (B-DNA) as mentioned above, but could equally be traced back to the difference in water content necessary for an alternative pathway. The independence of the activation gap from the humidity in the experiments of Tran *et al.* seems to favor the latter conclusion. We shall come back to the effects of the water solvent on the electronic states of DNA in Sec. V.B.

IV. THEORETICAL EFFORTS

Theoretical approaches can be divided into two classes: model calculations and *ab initio* (Hartree-Fock, DFT, and quantum molecular dynamics) calculations. The key limitation of the former is the uncertainty about which degrees of freedom and energy scales to include, since experiments do not give a conclusive picture, while the key difficulty of the latter is in handling the large unit cells.

We consider first theories for single charge transfer, which are much better developed. Model calculations are based upon the theory of Marcus (Marcus, 1956a, 1956b, 1993, 1998) and quantum master equations of the reduced density matrix (Schlag *et al.*, 2000). These have been used to describe single hole transfer in DNA. The essential ideas are as follows: in charge transfer, a charge donor complex is driven to an ionic or excited state by oxidation/reduction interactions with radicals (radiolysis) or light absorption (photolysis). The excited donor state is energetically comparable to a distant acceptor state. These donor and acceptor states are typically within a large molecular energy gap. In the Marcus theory of single-step transfer, when the donor and acceptor states are sufficiently close, quantum-mechanical tunneling can occur whenever molecular vibrational fluctuations bring them into resonance. In equilibrium, they are separated by a free-energy difference ΔG. The energy of a vertical (radiationless) transition between the Born-Oppenheimer surface for the state of the molecule with D-centered charge to the Born-Oppenheimer surface with A-centered charge is denoted λ and is called the *reorganization energy*. This is the necessary energy to bring the levels into resonance. It has in general an outer contribution from polarizing the solvent and an inner one originating from the molecule itself by adjusting bond lengths. If we assume simple parabolic Born-Oppenheimer energy surfaces for the donor and acceptor states with identical curvatures, the semiclassical Marcus theory rate is given by

$$k_{et}=\left(\frac{4\pi^2}{h}\right)H_{DA}^2(4\pi\lambda k_B T)^{-1/2}\exp\left(\frac{-(\Delta G-\lambda)^2}{4\lambda k_B T}\right). \tag{5}$$

Here H_{DA} is the electronic coupling between donor (D) and acceptor (A) and bears most of the dependence upon the donor-acceptor separation R. Often, this has been described by a simple exponential, $H_{DA}\sim\exp(-\beta R/2)$, where β is the inverse tunneling length. The exponential Boltzmann factor in Eq. (5) is the probability for reorganization of the environment in order to reach the transition state. The tunneling is through the bridging molecular medium between the donor and acceptor sites. Because this is a single quantum-mechanical event, it is said to be coherent charge transfer, and it is readily picked out by an exponential decay of the tunneling rate or its proxy (e.g., quenching of donor fluorescence) on the donor/acceptor distance. If the distance is too great, the excited charge will likely make it from donor to acceptor in an incoherent fashion, either by thermal activation (analogous to a semiconductor) or via multiple hops in the small-polaron limit. In this case, an algebraic dependence upon donor/acceptor separation will result.

Several mechanisms have been put forward for charge transfer in DNA. Depending on the DNA sequence and donor-bridge-acceptor energetics, one or a combination of the following may be applicable: (i) superexchange (McConnel, 1961; Kuznetsov and Ulstrup, 1998) or (ii) incoherent hopping (Jortner *et al.*, 1998; Bixon and Jort-

ner, 2000, 2001b). Superexchange of charge corresponds to a nearly atomic limit, in which the tunneling is treated perturbatively and H_{DA} scales like $\sim(t/\Delta)^N$, where t is the hopping between neighboring molecular subunits (i.e., the base pairs for DNA), Δ is the energy gap between the resonant donor energy and the LUMO (HOMO) for the molecular bridge for electron (hole) transfer, and N is the number of molecular units between donor and acceptor sites. Incoherent polaronlike hopping (Conwell and Rakhmanova, 2000; Rakhmanova and Conwell, 2001) may also be fluctuation-induced (Bruinsma *et al.*, 2000) or solvent-induced (Barnett *et al.*, 2001). (iii) Finally, bandlike transport has also been proposed as a possible explanation for weakly distance-dependent charge transfer under certain conditions (Grozema *et al.*, 2000). For a recent review of charge-transfer studies, the reader is referred to Bixon and Jortner (1999).

A conceptual problem through the 1990s was a controversy about how large the energy gap of DNA actually is. Barton's original work on long-range electron transfer in DNA (Murphy *et al.*, 1993) suggested a rather small gap ($\sim$2 eV), while early theoretical models assumed large gaps ($\sim$8 eV) based on Hartree-Fock theory (Priyadarshy *et al.*, 1996) and hence led to large deviations between theory and experiment. Hartree-Fock theory largely overestimates optical gaps (while the DFT method does the opposite). Experimentally, the dominant oscillator strength features a peak near 4 eV in the optical conductivity (Helgren *et al.*, 2002), close to experimental and theoretical estimates for single bases.

Let us now turn to the conductivity of DNA. Several theorists (Hjort and Strafström, 2001; Li and Yan, 2001; Cuniberti *et al.*, 2002; Feng and Xiong, 2002) have focused on Porath's clean-cut experiment on transport through homogeneous, 30-base-pair-long DNA (Porath *et al.*, 2000). They utilized standard scattering theory and the Landauer-Büttiker formula in order to explain the wide-gap I-V characteristics. The bottom line of these studies is that resonant tunneling with some degree of inelastic scattering or dephasing can explain the wide-gap and steplike I-V curves, as well as the peak broadening of the differential conductance. The large variations of the gap at different measurement sweeps and temperatures may be explained by a temperature-dependent modification of the base pair coupling and/or the coupling to the reservoirs (phonon bath, backbone, etc.). The conductivity measurements by Tran *et al.* (2000) and Yoo *et al.* (2001), showing a strong temperature dependence at high temperatures and a weak temperature dependence at low temperatures, were explained by Yu and Song (2000) and Cizek *et al.* (2003). They argued that activated hopping between neighboring bases at high T and variable-range hopping at low T, in combination with thermal structural fluctuations, gives good agreement with experiments. However, these theories are seriously incomplete in the following sense: unlike charge transfer, in which the origin of the electron/hole is clear through radiolytic or photolytic excitation, or in the field-effect transistors of Yoo *et al.* (2001) via voltage gating, the origin of the carriers in the low gap optical conductivity experiments is far from clear. Given the nominal $\simeq$4-eV optical gap for DNA (Helgren *et al.*, 2002), something must, in effect, dope the DNA in both of these experiments.

Two recent works have computed transmission coefficients in simplified models for different DNA sequences (Carpena *et al.*, 2002; Roche, 2003). The first work demonstrated that quasirandom sequences of DNA may in fact have longer-range correlation than expected, which can engender higher transmission for some states. The second considered the impact of leads and torsional fluctuations on transmission, as well as the role of quasirandom sequences of biological DNA (Roche, 2003). For periodic DNA, if the intrinsic DNA hopping is comparable to the lead-to-DNA tunneling matrix element, then within the well-defined DNA bands high transmission is possible, which is compatible with the observations of Porath *et al.* (2000). Reducing the ratio of base-to-base hopping relative to lead-to-base hopping and increasing the temperature (which induces torsional fluctuations) generally reduces the amplitude of transmission at all energies. Using quasirandom biological sequences uniformly reduces the transmission coefficient at all energies and seems to permit only a few sharp resonances.

In the remainder of this section we want to turn to *ab initio* methods aimed mostly at gaining insight into the electronic structure of DNA and its dependence on sequence, solvent, and counterions. Here the main difficulties arising are the large number of atoms ($\sim$1000 or more), inclusion of the solvent, and large thermal fluctuations. The first band-structure calculation on a canonical B-DNA structure without solvent was performed by Lewis *et al.* (1997) using the FIREBALL DFT code (Lewis *et al.*, 2001). These results were made feasible by the use of local orbitals (the Sankey-Niiklewski approach), pseudopotentials, and the implementation of a linear-scaling algorithm. A DFT code with similar features, SIESTA (Sánchez-Portal *et al.*, 1997), was also applied to calculate the band structure of a fully relaxed A-DNA structure, indicating an extremely small HOMO/LUMO bandwidth (de Pablo *et al.*, 2000).

For homogeneous sequences the unit cell can be reduced to a single base pair by using the following procedure. Bloch's theorem for periodic systems can be extended to helical systems by replacing a simple translation by a translation plus a rotation. For canonical B-DNA the values corresponding to this screw operation are 3.4 Å and 36°, respectively. This was first used for helical chain polymers, was applied to helical carbon nanotubes, and was then used to calculate the electronic structure of homogeneous DNA (Zhang *et al.*, 1999). However, the screw symmetry cannot be rigorously employed when solvent and counterions are present.

Very recently, the effects of solvent, counterions, and DNA dynamics have been addressed with *ab initio* methods (Endres *et al.*, 2002; Gervasio *et al.*, 2002; Lewis *et al.*, 2002). The FIREBALL code was used to understand the influence of DNA's dynamics on the electronic struc-

ture. While the canonical structure has rather extended states, structures from snapshots of classical molecular-dynamics simulations show localized states (Lewis *et al.*, 2002). Gervasio *et al.* (2002) achieved a breakthrough with the Carr-Parrinello molecular dynamics plane-wave code toward a fully *ab inito* quantum-molecular-dynamics simulation. The system they studied was the full 12-base-pair unit cell of left-handed Z-DNA, solvent, and sodium counterions. While the effects of solvent and counterions on DNA's molecular states are discussed in the next section, this calculation showed clearly that the solvent has to be included quantum mechanically. The full polarizability is necessary in order to account for different water patterns and dipole moments μ, both close to the DNA molecule (with gas-phase-like $\mu=1.7$ D) and far away from it (with bulklike $\mu=3.8$ D).

It has been further suggested that the dynamics of the counterions have a crucial impact on charge migration in DNA (Barnett *et al.*, 2001; Basko and Conwell, 2002). *Ab inito* methods on selected structures from a classical molecular-dynamics simulation show that counterions actually gate the single charge transport in DNA by adjusting the energy levels (Barnett *et al.*, 2001)—a reorganization already inherent in the classical theory of Marcus (1956a, 1956b, 1993, 1998). A recent *ab initio* study employing the SIESTA code on a singly charged (positive) segment of four-base-pair DNA found evidence of polaron formation with an estimated 0.15 eV gap for activated polaronic conduction (Alexandre *et al.*, 2003). The charged hole was placed in the bases, and the DNA segment was dry, without water or counterions (but with protons balancing the phosphate charge). The authors noted especially the agreement of this estimate with the zero-bias conductivity activation energy found by Yoo *et al.* (2001). However, the model calculations only apply to *doped* segments of DNA, and while Yoo *et al.* (2001) carried out field-effect doping in the second set of experiments reported in their paper, it is not apparent that the DNA bundles studied at zero bias were in fact doped. As noted in the schematic diagram of Fig. 5 of Yoo *et al.* (2001), without doping the states must be well within the DNA π-π^* gap, for which the binding energy is an order of magnitude larger than that calculated by Alexandre *et al.* (2003).

V. THE ROLE OF STRUCTURE AND ENVIRONMENT IN CONDUCTIVITY

A. Effects of DNA structure on π coupling

In this section, we first discuss the dependence of electronic states of DNA on its structure. Our motivation is to assess whether there are any structural conditions favorable to enhanced charge conduction along the π stack of the bases. In the presence of polar water molecules, DNA forms a double helix in order to protect the hydrophobic base pairs in its core region. There are several different helical structures dependent on the environment (humidity, salt type, and concentration) and whether it is under mechanical stress (molecular combing, gene transcription). Here we want to limit ourselves to the two main right-handed DNA conformations, the A- and B-DNA. The stretched DNA structure is discussed later in this section.

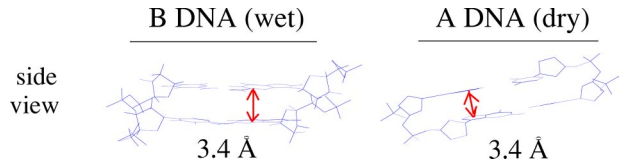

FIG. 6. (Color in online edition) Side view of two base pairs with backbones in the A and B forms. The B form is stable at high humidity. The base pair separation (indicated by arrows) of both A-DNA and B-DNA is about 3.4 Å. The backbones are to the left and right of the base pairs. Figure prepared with the program MOLMOL (Koradi *et al.*, 1996).

Biological DNA is mainly in B form, which is stable at more than 13 water molecules per nucleotide (Warman *et al.*, 1996). The base pairs have an average separation of about 3.4 Å and a relative twist angle of around 36° about the helical axis (Chandrasekaran and Arnott, 1996). The structure is very regular and the base pairs are well stacked (strong geometrical overlap). The A form, on the other hand, exists at lower humidity. However, at least about 5–10 water molecules are necessary to form a more or less regularly ordered A structure. Although the base pair separation and the twist angle are only 2.5 Å and 32.7° (Arnott and Hukins, 1972), the stacking is less effective. By *effective stacking* we mean that atomic p_z orbitals of atoms in neighboring base pairs overlap well or, more loosely, that any two successive base pairs overlap well. The canonical A- and B-DNA structures are shown in Figs. 6 and 7.

From Eq. (2) one expects that there will be more decent σ overlaps between atomic p_z orbitals from adjacent base pairs in B form than in A form. More importantly, competition between σ and π couplings can cancel the electronic coupling completely in A-DNA. This is demonstrated in Fig. 8, where a distribution of all possible interatomic matrix elements is shown [V_{ij} in Eq. (4)]. There are more good contacts, six times more above 0.5 eV, in the B form than in the A form. Furthermore, there is a shift to (negative) $pp\pi$ interaction in

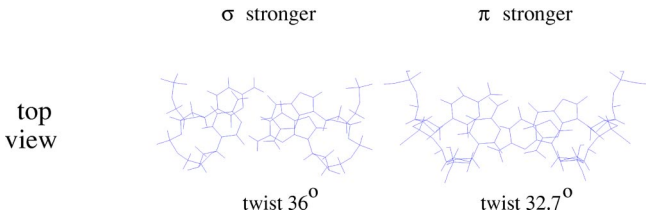

FIG. 7. (Color in online edition) Top view of two base pairs with backbones in the A and B forms. Although the twist angle is smaller for A-DNA, two successive base pairs in B form overlap better (are on top of each other). This is expected to result in more direct σ overlap between atomic p_z orbitals in the B form and more indirect π overlap in the A form. Figure prepared with the program MOLMOL (Koradi *et al.*, 1996).

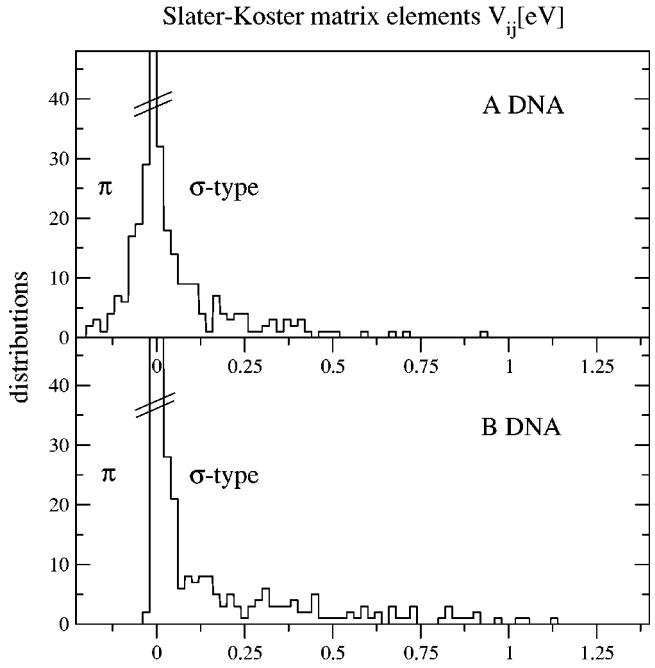

FIG. 8. Distribution of Slater-Koster interatomic matrix elements between p_z orbitals of two stacked G-C base pairs. There is a total of $19\times19=361$ matrix elements. A-DNA has more negative π interaction matrix elements.

the A form. The distribution of couplings for A-DNA is clearly more centered around zero than the distribution of B-DNA couplings. The latter is more asymmetric, with mostly positive matrix elements. The individual atomic interactions of A-DNA are small, as there are hardly any good σ contacts between any two atomic p_z orbitals (all matrix elements <1.0 eV). To be more precise, the inter-base-pair electronic coupling is the weighted average of these matrix elements, where the weights are the product of two LCAO coefficients. Since the LCAO coefficients stem from single-base-pair calculations and hence are very similar for A- and B-DNA, the coupling distribution clearly explains the small inter-base molecular-orbital couplings of A-DNA.

Instead of digging into this further we show in Fig. 9 the results of the π-π coupling t for various base pair dimers as calculated with the DFT code SIESTA (Ordejón *et al.*, 1996; Sánchez-Portal *et al.*, 1997; Artacho *et al.*, 1999; see also http://www.uam.es/siesta). One can immediately see that the couplings t are essentially zero for the A-DNA dimers. For further illustration we included two extra data points in the plot. One, GG (2.4 Å), corresponds to the B dimer GG but with the base pair separation reduced by 1 Å. This combines the good stacking property of B-DNA with a closer separation, resulting in large HOMO and LUMO couplings t. The other additional data point, GG (0°), shows the B dimer at zero twist angle about the axis normal to the base pair planes (instead of 36°). This leads to positive t's due to strong σ contacts.

There are other possible DNA structures that may result from mechanical stretching, for example, due to the use of the molecular combing technique (Parra and Windle, 1993; Bensimon *et al.*, 1995; Allemand *et al.*, 1997; Bustamante *et al.*, 2000). Molecular-dynamics simulations using classical force fields showed ribbonlike structures (Konrad and Bolonick, 1996; Lebrun and Lavery, 1996; Kosikov *et al.*, 1999) in this case. We explicitly examined whether a fully flat (base pairs and backbone all in one plane) structure might be driven metallic via potentially favorable base pair overlaps. However, we found, even allowing for this fully planar S-DNA structure, that the stretching only serves to localize the electronic states further due to a reduced number of good contacts (Endres *et al.*, 2002). This was recently confirmed by Maragakis and co-workers with a more extensive DFT calculation (Maragakis *et al.*, 2002).

These results may be relevant to some of the conductivity measurements. Drying DNA prior to the measure-

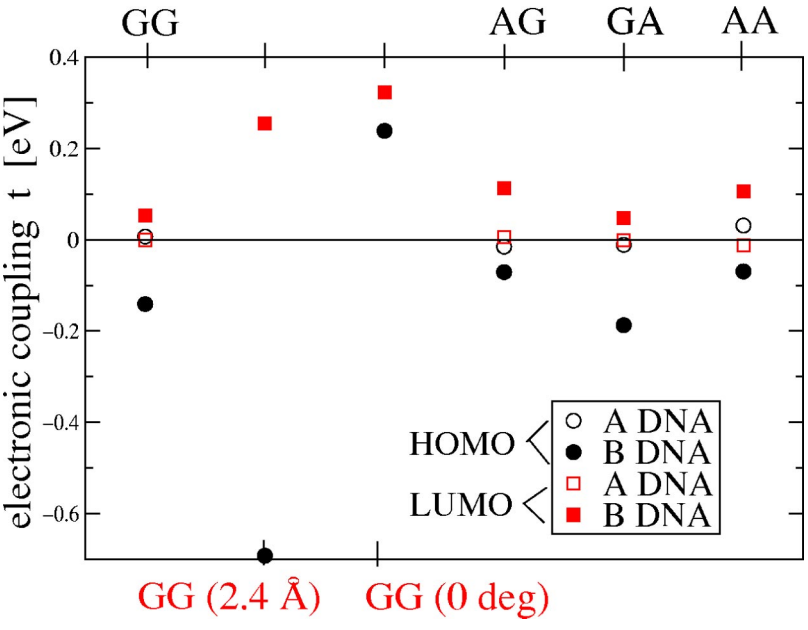

FIG. 9. (Color in online edition) Electronic couplings t in eV between HOMO's and LUMO's of two base pairs. GG stands for the dimer 5′-GG-3′ DNA.

ments may transform the DNA molecule into the A form. This structure has essentially zero π-π coupling strength. In some cases, as few as two to three water molecules per nucleotide have been reported (Tran *et al.*, 2000). This can even lead to distorted, irregular (Warman *et al.*, 1996) and hence fully insulating DNA. Similarly insulating behavior can arise for flat ribbonlike DNA structures resulting from molecular combing or possibly from binding to surfaces (Cai *et al.*, 2001). However, the case of bundles and supercoiled DNA could be different. It may be that a significant number of water molecules remain trapped between the DNA molecules of a bundle. This can help preserve the well-stacked B-DNA structure. In the next section, we address the question of whether the solvent and counterions can induce impurity states in the π-π^* gap of DNA, which could give rise to an activated hopping conductivity.

B. Impurity states and doping

From the discussions in the previous sections, it can be gleaned that no one has yet been able to identify any structural conditions favorable for low-activation-energy conduction through the π stack of DNA. In particular, the class 3 experiments of Tran *et al.* (2000) and Yoo *et al.* (2001), with activation energies of order 0.1 eV, are not understood. Consequently one can either assume these results were produced by some artifact of the experimental method or else consider the speculative possibility that the relevant conduction takes place *outside* the base pair stack. The fact that the contactless optical experiments on biological λ-DNA (Tran *et al.*, 2000) and the field-effect transistors made from periodic [poly(G)-poly(C) or poly(A)-poly(T) DNA] (Yoo *et al.*, 2001) give very similar results despite the radically different ambient environment, probe method, and base pair sequence suggests both that the small activation gap is robust and that its likely origin is outside the base sequence, which is, after all, quasiperiodic for λ-DNA. In particular, the low-activation-energy charge transport could be associated with the sugar/phosphate backbone, or with counterions and modified states of the water. We know of no definitive answers to settle this point, but here we report on some of our preliminary investigations which point to the latter possibility (i.e., states associated with the counterion and water).

The goal in this subsection is to identify candidate low-lying states associated with DNA to explain class 3 and class 4 experiments with either small activation gaps or metallic behavior. We do not discuss whether these states are sufficient to explain the low-activation-gap conductance data in these experiments. However, some plausible low-lying excitations *must* exist to explain the small (or absent) gaps in the class 3 and 4 experiments. The arguments presented derive from density-functional theory results in which we interpret the differences between Kohn-Sham eigenvalues as excitation energies. Strictly speaking, this is not true, except in the case of an *exact* DFT, for which the HOMO and LUMO energies will in fact be the exact ionization and affinity energies, respectively (Perdew *et al.*, 1982; Savin *et al.*, 1998). However, for approximate DFT's they might be a guide.

The phosphate groups of the DNA molecule are negatively charged. Hence positive protons or metal cations (counterions) are necessary to neutralize and stabilize DNA. Water also plays a crucial role. Hydrophobic forces make DNA form a double helix, and the polarity of the water molecules helps screen DNA's charges. We are interested in knowing whether the solvent or ions can lead to states in the main π-π^* energy gap of DNA (impurity states), and hence dope the DNA.

In order to address these questions we carried out a DFT calculation for a four-base-pair-long B-DNA sequence (5′-GAAT-3′; Endres *et al.*, 2002). We considered the case of a high (alkaline) *p*H value in which no protons are present to neutralize the DNA molecule. Instead, we compared different counterions (sodium, magnesium) and examined the "band structure" with and without water but keeping the DNA structure and counterion positions fixed. For wet DNA, we used ~200 water molecules, i.e., about 25 per nucleotide.

In order to identify the energetically important states near the Fermi energy, we projected the density of states (DOS) on the atomic p_z orbitals of the base pairs (π and π^* molecular orbitals), on the phosphates (PO_4), and on the sugars. For the wet DNA, we also examined the projected DOS of the water molecules and counterions and analyzed their geometrical distance relative to the DNA molecule as described below.

The projected DOS for the case of sodium counterions is shown in Fig. 10 and for the magnesium counterions in Fig. 11. Parts (a) and (b) contain the projected DOS of wet DNA, while (c) contains that for dry DNA. In part (a) the DNA and in part (b) the water states are shown. The color of the water states is determined by their proximity (<3.5 Å) to one of DNA's molecular groups (base pairs=red, phosphates=green, ions =yellow; blue, on the other hand, means all water states, and not near sugars). For instance, the contribution to a water state stemming from a water molecule that is closer than 3.5 Å away from a phosphate group is colored green.

Let us first discuss wet DNA. For both sodium and magnesium counterions, one observes a rather large π-π^* gap of order 2.2 eV, mainly between the guanine HOMO and the thymine LUMO. [When we project the density of states on a single base, we find a direct optical gap of about 3.7 eV due to intrabase π-π^* transitions, while for Z-DNA similar values were obtained for the full periodic structure with water (Gervasio *et al.*, 2002).] However, when the optical conductivity is measured, only the transition between HOMO's and LUMO's of the same base are visible since only these have large dipole transition matrix elements. The experimental optical gaps for these are $\lesssim$3.8 eV (Helgren *et al.*, 2002).

We note the appearance of energies associated with water and counterion orbitals in the π-π^* gap, which are in both cases rather close to the DNA LUMO, as shown in Figs. 10(a) and 11(a). Even more dramatic are the results of Figs. 10(b) and 11(b): in each case, the

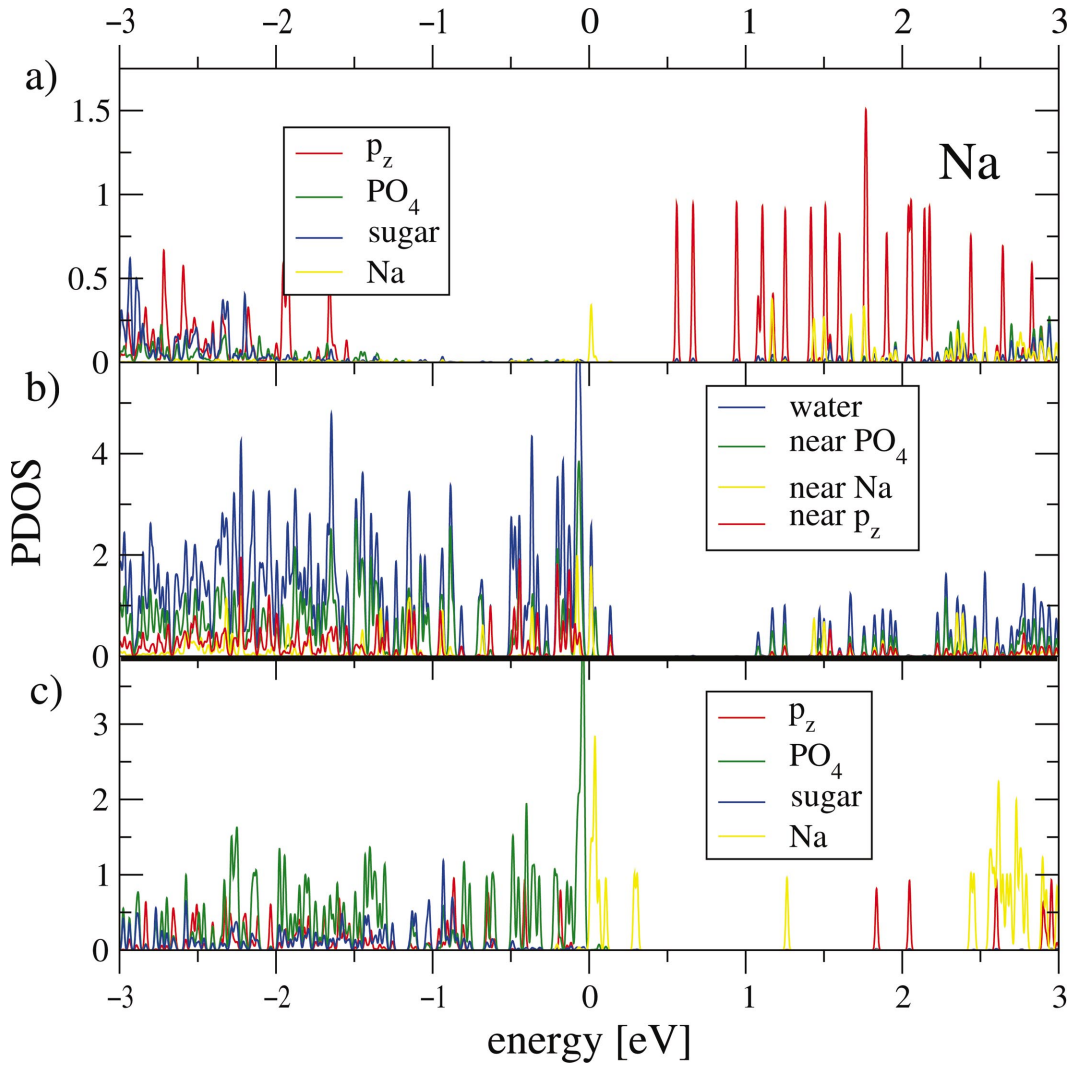

FIG. 10. (Color) Effects of sodium counterions and water on the molecular orbitals of four-base-pair-long B-DNA. Parts (a) and (b) show the projected DOS of wet DNA; (a) red, p_z (π); green, phosphate; blue, sugar; yellow, sodium; (b) blue, all water molecules; green, water molecules near phosphates (<3.5 Å); yellow, water molecules near sodium; red, water molecules near bases. In part (c) all the water molecules are removed (dry DNA). See text for further discussion.

charged environment around the DNA has produced a dramatic modification of the water p states, whose eigenvalues spill into the π-π^* gap almost up to the Na and Mg states. For sodium, we have small activation gaps (of a few k_BT) between water and sodium states, which could lead to hopping conductivity between Na-centered states. This could explain the conductivity measurements in DNA bundles (Tran *et al.*, 2000; Rakitin *et al.*, 2001; Yoo *et al.*, 2001) if enough water molecules are trapped between the DNA molecules. For magnesium, the occupied water state energies are not only close to the Mg levels [indeed, we find nominally Mg^+ rather than the expected Mg^{2+}, which has also been identified in DFT studies of Mg in water previously (Vicens and López, 2000)], they are also very close to the unoccupied π^* states, leading to the possibility of electron doping of DNA by water or Mg states. Whether this can explain the proximity effect below 1 K (Kasumov *et al.*, 2001) is unclear, especially since single nominally dry DNA molecules were used. Still, to maintain structural stability, a condensed hydration/counterion shell is likely necessary. These results of small activation gaps involving water are quite stunning, since normally water has a very large insulating gap. It suggests that the water states are very perturbed in the presence of charged DNA. This may be due to large Stark shifts associated with the highly polarized medium around the DNA. That the water dipole moments can be strongly modified was noted before (Gervasio *et al.*, 2002). Additionally, although a single water molecule has a large energy gap, the overall gap of water clusters and bulk water can be substantially smaller due to large fluctuations of individual water levels. For instance, the time-averaged electronic DOS of liquid water obtained from Car-Parrinello molecular-mechanics simulations shows a nonzero DOS in between the main HOMO and LUMO peaks (see Fig. 4 in Laasonen *et al.*, 1993). From this perspective it is thus surprising to find electronic water states in the DNA π-π^* gap. Experimental support for small electronic activation gaps involving the solvent

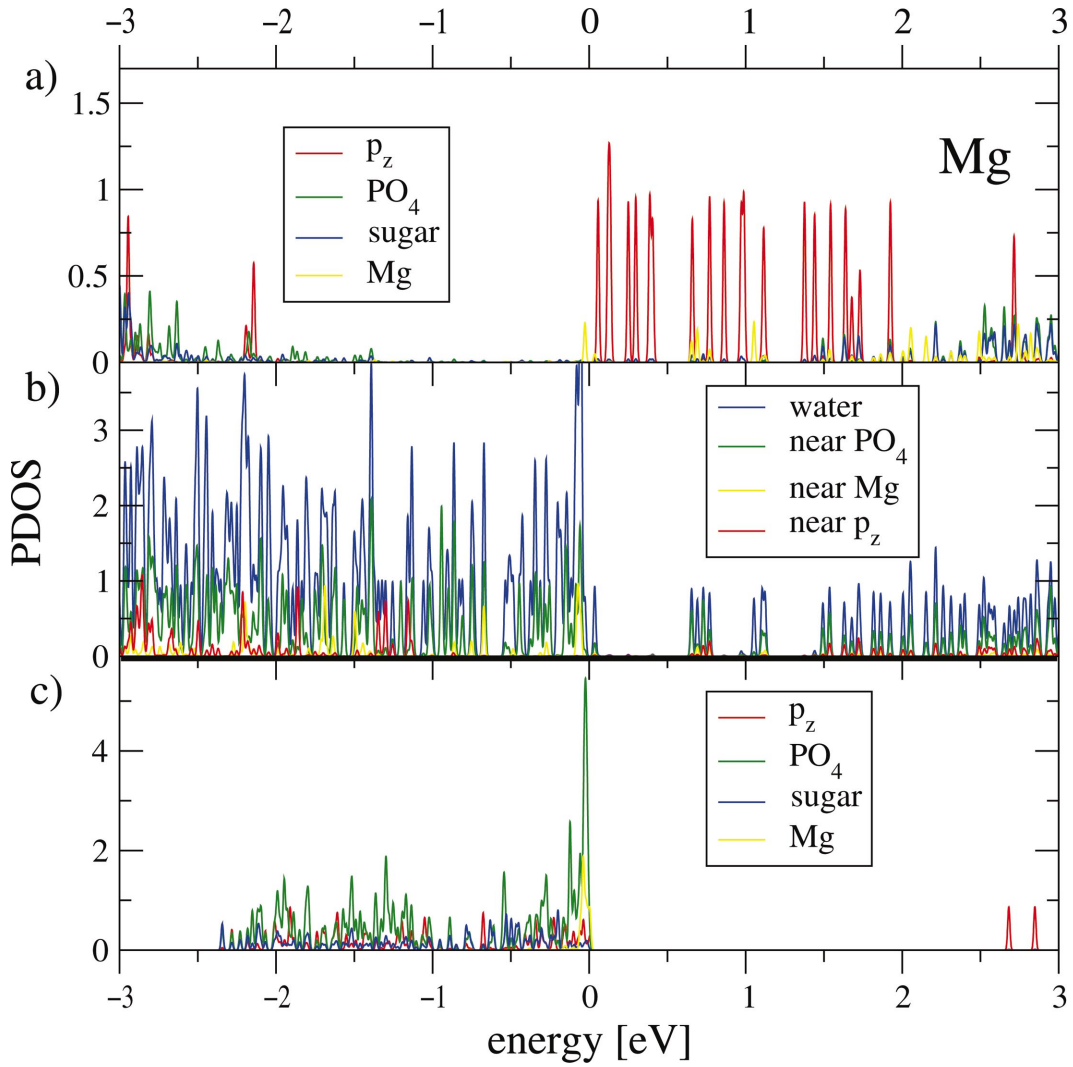

FIG. 11. (Color) Same as Fig. 10 except for magnesium counterions instead of sodium. Part (c): there is a single magnesium state just above the Fermi energy ($\epsilon_F=0$).

comes from ac conductance measurements by Briman *et al.* (2003) in the spectral range between 500 and 10 000 cm^{-1}. However, the authors suggested dipole relaxation losses as a possible cause for the small-activation-gap data. In their experiment a one to two orders of magnitude increase of the conductivity occurred when increasing the humidity from 0 to 84%. In addition, the conductivity was the same for single-stranded and double-stranded DNA and was not anisotropic. This clearly does not favor an electronic charge transport through the DNA base stack.

The calculated Mg^+ states are potentially rather remarkable. There is some experimental evidence for Mg^+, for example in the form of (i) clusters of Mg and n waters, with $n<5$ (Misaizu *et al.*, 1992; Reinhard and Nieder-Schatteburg, 2002) and (ii) transient states in slightly polar solvents (Renou and Mostafavi, 2001). This connection to the single molecules is intriguing because there will be relatively few water molecules around a given Mg ion. Also, in the transient flow around DNA captured only in snapshots in the calculations discussed here, such clustering conditions may exist. Hence, while the results presented are speculative in the sense of the relative difficulty of observing Mg^+, they are not without experimental support.

In part (c) of Figs. 10 and 11 the projected DOS of dry DNA is shown. Most interesting is the fact that the occupied phosphate states (green) are energetically higher than the occupied π states due to repulsive interactions between the negatively charged oxygens. This can be traced to the insufficient screening caused by the absence of water. The phosphate energy levels cannot, however, become higher than all empty metal states. If they were higher, the phosphates would donate electrons and would be able to lower their energy. If lower than the metal states, the metal ions would donate electrons back again, and the same process would start all over again. This process leads to pinning and hence a large density of states of phosphate orbitals right below empty metal ion states. Due to the extremely small gap between phosphate and counterion levels ($\sim k_B T$), one can imagine that hole doping of the backbone may be feasible. The backbone constitutes a quasi-one-dimensional periodic system which is essentially inde-

pendent of the base pair sequence and could allow for extended Bloch states. Nevertheless, conduction through the backbone remains questionable because of the insulating sugars separating phosphate groups from each other.

Clearly more studies will have to be done in order to obtain a reliable picture, since DFT calculations on systems containing ions with long-range Coulomb interactions are still quite challenging. Another question one must ask is: How well can potential solvent/backbone-impurity states of wet/dry DNA support actual transport?

VI. CONCLUSION

In this Colloquium we have presented an elementary introduction to the electronic properties of DNA. We began by discussing its similarities to certain charge-transfer molecular metals. We then summarized recent experimental and theoretical studies of electron transport in DNA. For migration of a single hole in DNA, a general theoretical consensus appears to be emerging. However, the conductance behavior of DNA remains poorly understood. Nevertheless, insights from *ab initio* methods do help explain some of the conflicting experimental outcomes. It appears that drying DNA—as is usually done prior to measuring the conductance—can lead to DNA conformations with localized electronic π states, although hole doping of the backbone by counterions might be possible. On the other hand, wet DNA may support electrical current, partly due to solvent impurity states sitting in the large π-π^* energy gap. In the case of divalent magnesium counterions, these might even electron-dope unoccupied π^* states.

Whether the "molecule of life" can also lead us into a second industrial revolution cannot yet be said. We are just at the beginning. The first DNA field-effect transistor has been built (Yoo *et al.*, 2001), and more DNA-based molecular electronic devices will likely follow.

ACKNOWLEDGMENTS

We would like to thank E. Artacho, P. Ordejón, D. Sánchez-Portal, and J. M. Soler for providing us with their *ab initio* code SIESTA. R.G.E. thanks R. Laughlin for providing temporary work space at Stanford University, where part of the writing was done. This work was supported by the U.S. Department of Energy, Office of Basic Energy Sciences, Division of Materials Research, and in the latter stages by the Center for Biophotonics, an NSF Science and Technology Center, managed by the University of California, Davis, under Cooperative Agreement No. PHY 0120999. This work was initiated with the assistance of a Seed Grant from the Materials Research Institute of Lawrence Livermore National Laboratories, and we ackowledge the use of the LLNL computer clusters in connection with this grant. At ORNL, R.G.E. acknowledges the support of DOE-OS through OASCR-MICS under Contract No. DE-AC05-00OR22725 with UT-Battelle LLC.

REFERENCES

Aflatooni, K., G. A. Gallup, and P. D. Burrow, 1998, J. Phys. Chem. A **102**, 6205.
Alexandre, S. S., E. Artacho, J. M. Soler, and H. Chacham, 2003, Phys. Rev. Lett. **91**, 108105.
Allemand, J. F., D. Bensimon, L. Jullien, A. Bensimon, and V. Croquette, 1997, Biophys. J. **73**, 2064.
Anderson, P. W., 1958, Phys. Rev. **109**, 1492.
Arnott, S., and D. W. L. Hukins, 1972, Biochem. Biophys. Res. Commun. **47**, 1504.
Artacho, E., D. Sánchez-Portal, P. Ordejón, A. Garcia, and J. M. Soler, 1999, Phys. Status Solidi B **215**, 809.
Ashcroft, N. W., and N. D. Mermin, 1976, *Solid State Physics* (Saunders College Publishing, Philadelphia), p. 364.
Bakknist, C. J., and M. B. Kastan, 2003, Nature (London) **421**, 499.
Barnett, R. N., C. L. Cleveland, A. Joy, U. Landman, and G. B. Schuster, 2001, Science **294**, 567.
Barrow, G. M., 1988, *Physical Chemistry*, 5th ed. (McGraw-Hill, New York), pp. 581–582.
Basko, D. M., and E. M. Conwell, 2002, Phys. Rev. Lett. **88**, 098102.
Bensimon, D., A. J. Simon, V. Croquette, and A. Bensimon, 1995, Phys. Rev. Lett. **74**, 4754.
Berlin, Y. A., A. L. Burin, and M. A. Ratner, 2000, Superlattices Microstruct. **28**, 241.
Bixon, M., and J. Jortner, 1999, Adv. Chem. Phys. **106**, 35.
Bixon, M., and J. Jortner, 2000, J. Phys. Chem. B **104**, 3906.
Bixon, M., and J. Jortner, 2001a, J. Am. Chem. Soc. **123**, 12556.
Bixon, M., and J. Jortner, 2001b, J. Phys. Chem. A **105**, 10322.
Braun, E., Y. Eichen, U. Sivan, and G. Ben-Yoseph, 1998, Nature (London) **391**, 775.
Brauns, E. B., M. L. Madaras, R. S. Coleman, C. J. Murphy, and M. A. Berg, 1999, J. Am. Chem. Soc. **121**, 11644.
Breslauer, K. J., R. Frank, H. Blöcker, and L. A. Marky, 1986, Proc. Natl. Acad. Sci. U.S.A. **83**, 3746.
Briman, M., N. P. Armitage, E. Helgren, and G. Grüner, 2003, e-print cond-mat/0303240.
Bruinsma, R., G. Grüner, M. R. D'Orsogna, and J. Rudnick, 2000, Phys. Rev. Lett. **85**, 4393.
Bustamante, C., S. B. Smith, J. Liphardt, and D. Smith, 2000, Curr. Opin. Struct. Biol. **10**, 279.
Cai, L., H. Tabata, and T. Kawai, 2000, Appl. Phys. Lett. **77**, 3105.
Cai, L., H. Tabata, and T. Kawai, 2001, Nanotechnology **12**, 211.
Carpena, P., P. Bernaola-Galván, P. Ch. Ivanov, and H. E. Stanley, 2002, Nature (London) **418**, 955.
Chandrasekaran, R., and S. Arnott, 1996, J. Biomol. Struct. Dyn. **13**, 1015.
Chen, J., and N. C. Seeman, 1991, Nature (London) **350**, 631.
Cizek, J., A. Martinez, and J. Ladik, 2003, THEOCHEM. **626**, 77.
Cocco, S., and R. Monasson, 2000, J. Chem. Phys. **112**, 10017.
Conwell, E. M., and S. V. Rakhmanova, 2000, Proc. Natl. Acad. Sci. U.S.A. **97**, 4557.
Cuniberti, G., L. Craco, D. Porath, and C. Dekker, 2002, Phys. Rev. B **65**, 241314(R).
Dandliker, P. J., R. E. Holmlin, and J. K. Barton, 1997, Science **275**, 1465.
Dekker, C., and M. A. Ratner, 2001, Phys. World **14** (8), 29.

de Pablo, P. J., F. Moreno-Herrero, J. Colchero, J. Gómez Herrero, P. Herrero, A. M. Bar, P. Ordejón, J. M. Soler, and E. Artacho, 2000, Phys. Rev. Lett. **85**, 4992.
Eley, D. D., and D. I. Spivey, 1962, Trans. Faraday Soc. **58**, 411.
Endres, R. G., D. L. Cox, and R. R. P. Singh, 2002, e-print cond-mat/0201404.
Feng, J.-F., and S.-J. Xiong, 2002, Phys. Rev. E **66**, 021908.
Fink, H. W., and C. Schönenberger, 1999, Nature (London) **398**, 407.
Friedberg, E. C., 2003, Nature (London) **421**, 436.
Gervasio, F. L., P. Carloni, and M. Parrinello, 2002, Phys. Rev. Lett. **89**, 108102.
Giese, B., J. Amaudrut, A. Köhler, M. Spormann, and S. Wessely, 2001, Nature (London) **412**, 318.
Gorin, A. A., V. B. Zhurkin, and W. K. Olson, 1995, J. Mol. Biol. **247**, 34.
Grozema, F. C., Y. A. Berlin, and L. D. A. Siebbeles, 2000, J. Am. Chem. Soc. **122**, 10903.
Hall, D. B., R. E. Holmlin, and J. K. Barton, 1996, Nature (London) **382**, 731.
Harrison, W. A., 1989, *Electronic Structure and the Properties of Solids* (Dover, New York), pp. 48 and 481.
Hartzell, B., B. McCord, D. Asare, H. Chen, J. J. Heremans, and V. Soghomonian, 2003a, Appl. Phys. Lett. **82**, 4800.
Hartzell, B., B. McCord, D. Asare, H. Chen, J. J. Heremans, and V. Soghomonian, 2003b, J. Appl. Phys. **94**, 2764.
Helgren, E., A. Omerzu, G. Grüner, D. Mihailovich, R. Podgornik, H. Grimm, 2002, e-print cond-mat/0111299.
Heller, A., 2000, Faraday Discuss. **116**, 1.
Henderson, P. T., D. Jones, G. Hampikian, Y. Kan, and G. B. Schuster, 1999, Proc. Natl. Acad. Sci. U.S.A. **96**, 8353.
Hjort, M., and S. Strafström, 2001, Phys. Rev. Lett. **87**, 228101.
Hodgman, C. D., and W. R. Veazey, 1966, *Handbook of Chemistry and Physics*, 47th ed. (The Chemical Rubber Co., Cleveland, 1966), p. E-68.
Jortner, J., M. Bixon, T. Langenbacher, and M. E. Michel-Beyerle, 1998, Proc. Natl. Acad. Sci. U.S.A. **95**, 12759.
Kasumov, A. Y., M. Kociak, S. Gueron, B. Reulet, and V. T. Volkov, 2001, Science **291**, 280.
Kelley, S. O., N. M. Jackson, M. G. Hill, and J. K. Barton, 1999, Angew. Chem., Int. Ed. Engl. **38**, 941.
Konrad, M. W., and J. I. Bolonick, 1996, J. Am. Chem. Soc. **118**, 10989.
Koradi, R., M. Billeter, and K. Wüthrich, 1996, J. Mol. Graphics **14**, 51.
Kosikov, K. M., A. A. Gorin, V. B. Zhurkin, and W. K. Olson, 1999, J. Mol. Biol. **289**, 1301.
Kuznetsov, A. M., and J. Ulstrup, 1998, *Electron Transfer in Chemistry and Biology: An Introduction to the Theory* (Wiley, Chichester).
Laasonen, K., M. Sprik, M. Parrinello, and R. Car, 1993, J. Chem. Phys. **99**, 9080.
Lebrun, A., and R. Lavery, 1996, Nucleic Acids Res. **24**, 2260.
Lewis, F. D., X. Y. Liu, J. Q. Liu, S. E. Miller, R. T. Hayes, and M. R. Wasielewski, 2000, Nature (London) **406**, 51.
Lewis, J. P., K. R. Glaesemann, G. A. Voth, J. Fritsch, A. A. Demkov, J. Ortega, and O. F. Sankey, 2001, Phys. Rev. B **64**, 195103.
Lewis, J. P., P. Ordejón, and O. F. Sankey, 1997, Phys. Rev. B **55**, 6880.
Lewis, J. P., J. Pikus, T. E. Cheatham, E. B. Starikov, H. Wang, J. Tomfohr, and O. F. Sankey, 2002, Phys. Status Solidi B **233**, 90.
Li, X.-Q., and Y. J. Yan, 2001, Appl. Phys. Lett. **79**, 2190.
Lias, S. G., J. E. Bartmess, J. F. Liebman, L. J. Holmes, R. D. Levin, and W. G. Mallard, 1988, J. Phys. Chem. Ref. Data **17**, (Suppl. 1), 1–861.
Misaizu, F., M. Sanekata, K. Tsukamoto, K. Fuke, and S. Iwata, J. Phys. Chem. **96**, 8259.
Maragakis, P., R. L. Barnett, E. Kaxiras, M. Elstner, and T. Frauenheim, 2002, Phys. Rev. B **66**, 241104(R).
Marcus, R. A., 1956a, J. Chem. Phys. **24**, 966.
Marcus, R. A., 1956b, J. Chem. Phys. **24**, 979.
Marcus, R. A., 1993, Rev. Mod. Phys. **65**, 599.
Marcus, R. A., 1998, J. Phys. Chem. B **102**, 10071.
McConnell, H. M., 1961, J. Chem. Phys. **35**, 508.
Murphy, C. J., M. R. Arkin, Y. Jenkins, N. D. Ghatlia, S. H. Bossmann, N. J. Turro, and J. K. Barton, 1993, Science **262**, 1025.
Olson, W. K., and V. B. Zhurkin, 2000, Curr. Opin. Struct. Biol. **10**, 286.
Ordejón, P., E. Artacho, and J. M. Soler, 1996, Phys. Rev. B **53**, R10441.
Orlov, V. M., A. N. Smirnov, and T. M. Varshavsky, 1976, Tetrahedron Lett. **48**, 4377.
Parra, I., and B. Windle, 1993, Nat. Genet. **5**, 17.
Perdew, J. P., R. G. Parr, M. Levy, and J. L. Balduz, Jr., 1982, Phys. Rev. Lett. **49**, 1691.
Porath, D., A. Bezryadin, S. De Vries, and C. Decker, 2000, Nature (London) **403**, 635.
Priyadarshy, S., S. M. Risser, and D. N. Beratan, 1996, J. Phys. Chem. **100**, 17678.
Rajski, S. R., B. A. Jackson, and J. K. Barton, 2000, Mutat Res. **447**, 49.
Rakhmanova, S. V., and E. M. Conwell, 2001, J. Phys. Chem. B **105**, 2056.
Rakitin, A., P. Aich, C. Papadopoulos, Y. Kobzar, A. S. Vedeneev, J. S. Lee, and J. M. Xu, 2001, Phys. Rev. Lett. **86**, 3670.
Reinhard, B. M. and G. Niedner-Schatteburg, 2002, Phys. Chem. Chem. Phys. **4**, 1471.
Renou, F., and M. Mostafavi, 2001, Chem. Phys. Lett. **335**, 363.
Roche, S., 2003, Phys. Rev. Lett. **91**, 108101.
Roth, S. R., 1995, *One-Dimensional Metals,* 1st ed. (VCG Verlagsgesellschaft, Weinheim, Germany), pp. 31–35 and 116.
Sánchez-Portal, D., P. Ordejón, E. Artacho, and J. M. Soler, 1997, Int. J. Quantum Chem. **65**, 453.
Savin, A., C. J. Umrigar, and X. Gonze, 1998, Chem. Phys. Lett. **288**, 391.
Schlag, E. W., D.-Y. Yang, S.-Y. Sheu, H. L. Selzle, S. H. Lin, and P. M. Rentzepis, 2000, Proc. Natl. Acad. Sci. U.S.A. **97**, 9849.
Seidel, C. A. M., A. Schulz, and M. H. M. Sauer, 1996, J. Phys. Chem. **100**, 5541.
Sinden, R. R., 1994, *DNA Structure and Function* (Academic, San Diego).
Slater, J. C., and G. F. Koster, 1954, Phys. Rev. **94**, 1498.
Steenken, S., and S. V. Jovanovic, 1997, J. Am. Chem. Soc. **119**, 617.
Storm, A. J., J. van Noort, S. de Vries, and C. Dekker, 2001, Appl. Phys. Lett. **79**, 3881.
Sugiyama, H., and I. Saito, 1996, J. Am. Chem. Soc. **118**, 7063.
Thouless, D. J., 1977, Phys. Rev. Lett. **39**, 1167.
Tran, P., B. Alavi, and G. Grüner, 2000, Phys. Rev. Lett. **85**, 1564.
Vicens, M. C., and G. E. López, 2000, J. Comput. Chem. **21**, 64.

Wan, C., T. Fiebig, S. O. Kelley, C. R. Treadway, J. K. Barton, and A. H. Zewail, 1999, Proc. Natl. Acad. Sci. U.S.A. **96**, 6014.
Wan, C., T. Fiebig, O. Schiemann, J. K. Barton, and A. H. Zewail, 2000, Proc. Natl. Acad. Sci. U.S.A. **97**, 14052.
Warman, J. M., M. P. de Haas, and A. Rupprecht, 1996, Chem. Phys. Lett. **249**, 319.
Watson, J., and F. Crick, 1953, Nature (London) **171**, 737.
Wetmore, S. D., R. J. Boyed, and L. A. Eriksson, 2000, Chem. Phys. Lett. **322**, 129.
Yoo, K.-H., D. H. Ha, J.-O. Lee, J. W. Park, J. Kim, J. J. Kim, H.-Y. Lee, T. Kawai, and H. Y. Choi, 2001, Phys. Rev. Lett. **87**, 198102.
Young, M. A., G. Ravishanker, and D. L. Beveridge, 1997, Biophys. J. **73**, 2313.
Yu, Z. G., and X. Song, 2000, Phys. Rev. Lett. **86**, 6018.
Zhang, M.-L., M. S. Miao, V. E. Van Doren, J. J. Ladik, and J. W. Mintmire, 1999, J. Chem. Phys. **111**, 8696.
Zhang, Y., R. H. Austin, J. Kraeft, E. C. Cox, and N. P. Ong, 2002, Phys. Rev. Lett. **89**, 198102.
Zhang, Y., and N. C. Seeman, 1994, J. Am. Chem. Soc. **116**, 1661.